Hydrogen and carbon isotope fractionation in modern plant wax n-alkanes from the Falkland **Islands** Megan C. Corcoran a*, Aaron F. Diefendorf a, Thomas V. Lowell a, Brenda L. Hall b, Meghan M. Spoth b, Anna Schartman^c and Paul Brickle d,e ^a Department of Geology, University of Cincinnati, Cincinnati, OH 45221-0013, USA ^b School of Earth and Climate Sciences, University of Maine, Orono, ME 04469-5790, USA ^c Department of Ocean Sciences, University of California, Santa Cruz, Santa Cruz, CA 95064, USA ^d South Atlantic Environmental Research Institute, Stanley, Falkland Islands FIOO 1Z ^e School of Biological Sciences (Zoology), University of Aberdeen, Tillydrone Avenue, Aberdeen, Scotland AB24 2TZ, UK *Corresponding author. *E-mail address*: megcorcor@gmail.com (M. C. Corcoran) Declaration of interests: none. Corcoran, M. C., Diefendorf, A. F., Lowell, T. V., Hall, B. L., Spoth, M. M., Schartman, A., & Brickle, P. (2022). Hydrogen and carbon isotope fractionation in modern plant wax n-alkanes from the Falkland Islands. Organic Geochemistry, 166, 104404. https://www.sciencedirect.com/science/article/pii/S0146638022000389

27 ABSTRACT

28

29

30

31

32

33

34

35

36

37

38

39

40

41

42

43

44

The hydrogen isotopic composition of terrestrial plant waxes ($\delta^2 H_{wax}$) is widely used to reconstruct past hydroclimate. $\delta^2 H_{wax}$ reflects source water $\delta^2 H$, or precipitation $\delta^2 H$, and when extracted from sediment archives, records of past $\delta^2 H_{precip}$ can be generated. In order to better interpret these $\delta^2 H_{wax}$ records in the past, modern calibrations between plant waxes and source water are required when vegetation and location diverge greatly from prior plant calibrations in other regions. To date, no study has yet to examine how $\delta^2 H_{wax}$ and source water $\delta^2 H$ relate in the southern mid- and high-latitude maritime climatic regions. The cold maritime climate of the Falkland Islands is affected by the Southern Hemisphere Westerly Wind Belt, providing a unique opportunity to explore how the hydrological cycle responds to changes in the spatial extent of this atmospheric-oceanic system. We present the first modern calibration of $\delta^2 H_{\text{wax}}$ on the Falkland Islands by analyzing *n*-alkanes from 11 of the most common plant species, 1 lichen species and 5 surface lake sediments from four sites on Mount Usborne (705 msl) on East Falkland for plant wax concentrations, δ^2 H and δ^{13} C. We calculate the fractionation between the C_{29} *n*-alkane $\delta^2 H_{\text{wax}}$ and $\delta^2 H_{\text{precip}}$ ($\epsilon^2 H_{\text{wax/precip}}$) for all plant species to be $-110 \pm 17\%$ (1σ , n = 22), which is similar to the global average $\epsilon^2 H_{wax/precip}$. Observed and modelled monthly $\delta^2 H_{precip}$ indicate that $\delta^2 H_{wax}$ reflects mean annual $\delta^2 H_{precip}$, ultimately improving interpretations of plant wax-based paleoreconstuctions from the mid-latitude maritime climatic regions.

45

46

47 **Keywords:** Hydrogen isotopes, plant wax, *n*-alkanes, fractionation, terrestrial biomarkers, Falkland

48

Islands

50

49

1. Introduction

53

54

55

56

57

58

59

60

61

62

63

64

65

66

67

68

69

70

71

72

73

74

75

76

52

Understanding how the hydrological cycle changes during periods of rapid warming similar to today's climate is essential. The hydrogen isotopic composition ($\delta^2 H$) of plant waxes is often used to track and reconstruct global hydroclimate (Sachse et al., 2012; Freimuth et al., 2017). During wax synthesis, terrestrial plants utilize hydrogen from plant source water (e.g. soil water), which is sourced from precipitation falling onto the landscape (Sachse et al., 2012). The δ^2 H of terrestrial plant wax $(\delta^2 H_{\text{wax}})$ *n*-alkanes, typically long chained *n*-alkanes, therefore reflects precipitation $\delta^2 H$ ($\delta^2 H_{\text{precip}}$) (Tipple and Pagani, 2013). Records of $\delta^2 H_{wax}$, when extracted from lake sediment archives, can be used to infer past $\delta^2 H_{precip}$ and used to understand precipitation seasonality, precipitation amount and effective precipitation changes through time (Sachse et al., 2012; Feakins et al., 2016; Freimuth et al., 2017; Rach et al., 2017; Balascio et al., 2018; Thomas et al., 2020). In order to generate these records of $\delta^2 H_{\text{precip}}$ using $\delta^2 H_{\text{wax}}$, the fractionation between $\delta^2 H_{\text{precip}}$ and $\delta^2 H_{\text{wax}}$ ($\epsilon^2 H_{\text{wax/precip}}$) is needed (Sachse et al., 2012; Liu and An, 2019; McFarlin et al., 2019). $\varepsilon^2 H_{\text{wax/precip}}$ can vary spatially across latitudes, between plant taxonomic groups and among plants of the same species (Hou et al., 2007; Feakins and Sessions, 2010; McInerney et al., 2011; Duan and Xu, 2012; Sachse et al., 2012; Elev et al., 2014; Berke et al., 2019). This variation has been linked to differences in plant wax formation relating to plant source water, root depth, plant growth form and metabolic processes (Williams and Ehleringer, 2000; Sachse et al., 2012; Freimuth et al., 2017; Freimuth et al., 2019; Dion-Kirschner et al., 2020). Constraining $\varepsilon^2 H_{\text{wax/precip}}$ is challenging, because sediment archives represent a mixture of waxes derived from the catchment vegetation, where plants in the catchment make different amounts of waxes and various plant taphonomic controls result in only some waxes making it into the lake (Freimuth et al., 2019). Modern calibrations exploring the relationship between $\delta^2 H_{precip}$ and $\delta^2 H_{wax}$ at local and regional scales where vegetation and climate are unique and understudied are needed for accurate reconstructions of $\delta^2 H_{precip}$ and ultimately past hydroclimate

(Feakins and Sessions, 2010; Feakins et al., 2016; Daniels et al., 2017; Berke et al., 2019; Liu and An, 2019; He et al., 2020). To date, multiple studies have examined $\varepsilon^2 H_{wax/precip}$ between $\delta^2 H_{wax}$ and source water $\delta^2 H$ across the tropics (Feakins et al., 2016), mid-latitudes in the Northern Hemisphere (Sachse et al., 2004; Smith and Freeman, 2006; Kahmen et al., 2013; Tipple and Pagani, 2013; Freimuth et al., 2019; Freimuth et al., 2020) and the Arctic (Wilkie et al., 2013; Daniels et al., 2017; Berke et al., 2019; Dion-Kirschner et al., 2020; O'Connor et al., 2020). However, no studies yet exist to document $\varepsilon^2 H_{wax/precip}$ for mid- or high-latitudes in the Southern Hemisphere (Liu and An, 2019). This study targets plant wax and source water in Falkland Islands, located in the southern mid-latitudes close to the southern polar front. Here, vegetation consists of herbs, grasses and shrubs, which contrasts with other calibration studies at these latitudes in the northern hemisphere which are primarily made up of trees, but, aligns with Arctic calibrations of shrubs and grasses (Daniels et al., 2017; Berke et al., 2019; McFarlin et al., 2019; Dion-Kirschner et al., 2020; O'Connor et al., 2020). This study establishes a framework of interpreting modern plant waxes and source water in the Falkland Islands with the goal of future paleoclimate work in this region.

The Falkland Islands (52° S, 61° W) are located about 520 km east off of the coast of southern South America. Hydroclimate of the Falklands Islands is influenced by the Southern Hemisphere Westerlies (SHW), a complex atmospheric-oceanic system that is predicted to shift both in locality and intensity as climate changes (Russell et al., 2006; Kitoh et al., 2011; Chavaillaz et al., 2013). Latitudinal shifts in the SHW can cause changes in the moisture source and amount for regions such as the Falkland Islands that are in the path of the SHW (Anderson et al., 2009; Fletcher and Moreno, 2012). Modern observations of Falkland Islands' plants in a climate-controlled experiment have found that small increases in temperature has resulted in decreased soil moisture and ultimately more stressed conditions for grasses (Bokhorst et al., 2007). This implies that local ecosystems on the Falkland Islands are sensitive to any changes in moisture, including precipitation amount. Past records of moisture source and amount are therefore needed to constrain the direction and intensity of the SHW shifts in the future to

ultimately understand how ecosystems in the Falkland Islands and surrounding regions may be affected (Wyrwoll et al., 2000; Toggweiler et al., 2006; Rojas et al., 2009; Fletcher and Moreno, 2012). Records of $\delta^2 H_{precip}$ can be generated from sediment archives, however, in order to make use of sediment archives within the Falkland Islands and other sub-Antarctic and high-mid-latitude southern regions, and reconstruct $\delta^2 H_{wax}$, the local $\epsilon^2 H_{wax/precip}$ must be determined (Spoth et al., 2020).

Here, we compare $\delta^2 H_{wax}$ and $\delta^2 H_{precip}$ from 11 of the most common plant species and surface lake sediments from the Falkland Islands to determine the local average $\epsilon^2 H_{wax/precip}$. We use *n*-alkane concentrations, average chain length, and carbon ($\delta^{13} C_{wax}$) and hydrogen isotopes of plant wax *n*-alkanes to infer which plants contribute the most to Falkland lake sediments. Water systematics including $\delta^2 H_{precip}$, lake water $\delta^2 H$, leaf water $\delta^2 H$ ($\delta^2 H_{lw}$), and xylem water $\delta^2 H$ ($\delta^2 H_{xw}$) on the Falkland Islands are established from this region. Determining the $\epsilon^2 H_{wax/precip}$ of terrestrial plants on the Falkland Islands provides a framework for paleoclimate reconstructions of $\delta^2 H_{precip}$ using $\delta^2 H_{wax}$, ultimately aiding in the understanding of how hydroclimate and the SHW have shifted in the past.

2. Methods

2.1 Site information

The Falkland Islands is composed of two main islands, East and West Falkland, as well as more than 200 small surrounding islands (Moore, 1968). This study focuses on East Falkland, which is approximately 5,000 km², and contains a central mountain range with Mt. Usborne (705 m, ~75 m from capital of the Falkland Islands, Stanley) (Fig. 1a) (Moore, 1968). ¹⁰Be surface exposure dating of moraine boulders in this region indicate that glaciers occupied the cirques periodically throughout the last glacial cycle from at least 45 ka to 19 ka (Hall et al., 2020). Radiocarbon dating of the lowest organic remains in

sediment cores indicate that two of the tarns examined in this study, Tarns 2 (~600 m elevation) and 4 (~520 m elevation), were deglaciated by at least ~13.5 ka and 23 ka, respectively (Spoth et al.,2020).

The Falkland Islands have a cool oceanic climate with some seasonal variation in temperature (Fig. 1b, c, d) (Moore, 1968; Lister and Jones, 2015). Modern climate datasets for the Falkland Islands were obtained from the closest NOAA National Climatic Data Center station at Mount Pleasant (71 msl) in East Falkland (Fig. 1a) covering 1985 – 2019 (NOAA, 2021). Average monthly temperatures for all years of available data range from 1.8 °C and 9.7 °C between July and January (Fig. 1c) (NOAA, 2021). Average monthly precipitation amount for all years of available data ranges from 29 mm in October to 59 mm in December with an annual average precipitation amount of about 530 mm (Fig. 1d) (NOAA, 2021). Cloud coverage in the Falklands is frequent with roughly 75% cloud cover each month (Moore, 1968) and fog generally covers much of the region. Regional monthly precipitation isotopes were determined from both measured values from the closest Global Network of Isotopes in Precipitation (GNIP) station to the study site, Stanley (IAEA/WMO, 2020), and from modelled precipitation from the Online Isotopes in Precipitation Calculator (OIPC) at each study site (Fig. 1a, b) (Bowen and Revenaugh, 2003; Bowen, 2021; IAEA/WMO, 2021). Monthly precipitation samples were also collected on the Falkland Islands for one year at Cape Dolphin, West Point Island, and Surf Bay in 2015 by Groff et al. (2020) and are archived on GNIP (Fig. 1a). We report only the observed precipitation isotopes in Section 3.4 at Stanley because it spans multiple years.

144

126

127

128

129

130

131

132

133

134

135

136

137

138

139

140

141

142

143

2.2 Collection of plant and sediment samples

146

147

148

149

150

151

145

The native flora of the Falkland Islands includes about 170 vascular plant species with major vegetation types including acid grasslands and dwarf shrub heathlands (Broughton and McAdam, 2002). The two species that dominate these habitats are whitegrass, *Cortaderia pilosa*, and the shrub diddle-dee, *Empetrum rubrum* (Broughton and McAdam, 2002). We collected 27 plant samples from eastern Falkland from cirques occupied by tarns or small mountain lakes located on the northern flank of Mt.

Usborne in March of 2019 (Fig. 1e). We collected 11 plants species, including *C. pilosa* and *E. rubrum* (Fig. 1e). Plant samples were obtained from four different locations in close proximity to the tarns, two neighboring Black Tarn, one next to Tarn 2, and one next to Tarn 4 (Fig. 1e). Leaves were gathered from each plant species, which included woody shrubs, graminoids, ferns and forbs. A lichen, was also collected at Tarn 2. See Appendix A. Supplementary Table S1 and Fig. 2 for details of plant names and which plants were sampled from each of the four sites. All leaves were collected in paper bags, frozen and freeze-dried prior to analysis.

We obtained a total of five surface sediments (top 0.5 cm) from Tarns 2 and 4 using a UniCorer percussion corer and polycarbonate tubing. Sediments were extracted from the deepest parts of the lake basins (5 m water depth for Tarn 2 and 13.3 m for Tarn 4), as determined from bathymetric soundings.

2.3 Extraction, lipid assignment and quantification of plant wax n-alkanes

All collected plants samples were freeze dried. About 500 mg of homogenized leaves were extracted using an accelerated solvent extraction (ASE; Dionex 350) with 9:1 (v/v) hexanes/dichloromethane (DCM) using three extraction cycles at 10.3 MPa and 100 °C. The aliphatic fraction was separated from the total lipid extract using a 9:1 (v/v) hexanes/DCM mixture over silica gel. The aliphatic fraction was further separated into saturated and unsaturated compounds using hexanes and ethyl acetate, respectively, over 5% silver nitrate impregnated silica gel. The saturated aliphatic fraction was analyzed for *n*-alkanes.

n-Alkanes were identified and quantified on an Agilent 7890A gas chromatograph (GC) and Agilent 5975C quadrupole mass selective detector (MSD) and quantified using a flame ionization detector (FID) following the procedure found in Freimuth et al., 2020. Prior to quantification, all samples were spiked with 25 μg ml⁻¹1,1′-binaphthyl as an internal standard. Compound peak areas were first normalized to those of 1,1′-binaphthyl and then converted to concentration using response curves of *n*-alkanes (C₇ to C₄₀; Sigma Aldrich), also normalized to 1-1′-binaphtyl, ranging from 2.8 to 69.5 μg ml⁻¹.

n-Alkane precision and accuracy were determined on an in-house n-alkane standard (C_{29} and C_{31}) prepared from oak leaves (Oak-1a) which had a weighted mean precision of 1.6 μ g mL⁻¹ (1σ ; 2.0% relative standard deviation, RSD) and an accuracy of -2.0μ g mL⁻¹ (-2.5% relative error, RE). Compound concentrations were normalized to the dry leaf mass (μ g g⁻¹).

To compare *n*-alkane chain lengths between species, average chain length (ACL) was calculated using:

$$ACL_{m-n} = \sum_{i=m}^{n} \frac{i[C_i]}{[C_i]}$$
 Eq. 1

where m and n represent the shortest and longest chain length, respectively, i represents the number of carbon atoms for each homologue, and C is the concentration of the i n-alkane. We use odd n-alkane chain lengths from C_{25} and C_{37} .

2.4 n-Alkane isotopic analysis

The $\delta^2 H$ of the *n*-alkanes was determined using a Thermo Trace GC Ultra coupled to an Isolink pyrolysis reactor (1420 °C) and interfaced to a Thermo Electron Delta V Advantage IRMS via a Conflo IV following the GC oven program described in Freimuth et al., 2019, 2020. The H_3^+ factor was tested daily and averaged 2.9 ppm nA^{-1} during the period of analysis. The $\delta^2 H$ and $\delta^{13} C$ of the *n*-alkanes was normalized to the VSMOW/SLAP scale and VPDB scale, respectively, using periodic interspersed *n*-alkane standards of known $\delta^2 H$ and $\delta^{13} C$ composition (Mix A6, A. Schimmelmann, Indiana University) are are reported in delta notation (in units of per mil, ‰). An in-house standard, Oak-1a, was analyzed every ~8 samples with a pooled precision of 4.1‰ (n = 34) for $\delta^2 H$ and 0.2‰ (n = 40) for $\delta^{13} C$ for *n*-C₂₉ and *n*-C₃₁ alkanes. Long term analytical precision was determined by pooling the standard deviation from all replicates following Polissar and D'Andrea (2014) and was 2.8‰ for $\delta^2 H$ and 0.1‰ for $\delta^{13} C$.

2.5 Water sampling and isotopic analysis

Water samples (n=6) were collected from the Black Tarn, as well as from its outlet and from a small adjacent pool floored by peat, from Tarns 2 and 4, and from another smaller pond at lower elevation (Table 1) during March of 2019 using 30 mL Nalgene bottles. One river sample was collected near the sampled lakes (Table 1). Plant material was collected from all studied species except *E. rubrum* for leaf water analysis (n = 13) and from *B. magellanica* (n = 2) and *E. rubrum* (n = 2) for xylem water analysis in summer 2019. *B. magellanica* and *E. rubrum* were the only two plants that had woody tissue, allowing for analysis of xylem water. Plant sampling methods follow the established procedure in Freimuth et al. (2017).

Leaf and xylem water were extracted using cryogenic vacuum distillation following the established procedures in West et al., (2006) and (Freimuth et al., 2019). Exetainer vials containing the stem and leaves were evacuated to a pressure <8 Pa (<60 Torr), isolated from the vacuum pump and then heated to 100 °C. Water vapor was collected in borosilicate test tubes immersed in liquid nitrogen for at least 60 minutes. Collected water samples were thawed and transferred to a 2mL crimp-top vial and refrigerated until analysis.

Xylem water, leaf water, and lake water samples were analyzed for δ^2H and $\delta^{18}O$ using headspace equilibration using methods previously established (Paul and Skrzypek, 2006; Freimuth et al., 2020). The equilibrated headspace gases were analyzed on a Thermo Delta V Advantage IRMS with a Thermo Gasbench II with the IRMS connected to the IRMS with a Conflo IV interface. Volatile organics were removed from the sample via a liquid nitrogen trap. All samples were then normalized to the VSMOW/SLAP scale using three in-house standards (previously calibrated with VSMOW2, SLAP2, and GISP). Water precision and accuracy were 0.4‰ and -0.3% for $\delta^{18}O$ and 2.6% (n=16) and -1.4% (n=16) for δ^2H , respectively.

2.6 Calculation of fractionation between n-alkanes and source water

Fractionation (ϵ) between *n*-alkanes ($\delta^2 H_{wax}$) and source water was calculated using $\delta^2 H_{lw}$, $\delta^2 H_{xw}$, and $\delta^2 H_{precip}$. $\delta^2 H_{precip}$ was determined using the OIPC (v3.1) modelled precipitation isotopes (Bowen and Revenaugh, 2003; Bowen, 2021; IAEA/WMO, 2021). Mean annual precipitation values were assigned based on the OPIC $\delta^2 H_{precip}$ values. The following equation was used to calculate the fractionation between $\delta^2 H_{wax}$ and $\delta^2 H_{precip}$ or $\epsilon^2 H_{wax/precip}$.

235
$$\varepsilon^2 H_{wax/precip} = \left(\frac{\delta^2 H_{wax} + 1000}{\delta^2 H_{precip} + 1000}\right) - 1$$
 Eq. 2

 $\epsilon^2 H_{wax/precip}$ for each individual carbon chain length is defined as $\epsilon^2 H_{27/precip}$, $\epsilon^2 H_{29/precip}$, $\epsilon^2 H_{31/precip}$, and $\epsilon^2 H_{33/precip}$ for n-C₂₇, n-C₂₉, n-C₃₁, and n-C₃₃ alkanes, respectively. Fractionation between $\delta^2 H_{lw}$ and $\delta^2 H_{xw}$ ($\epsilon^2 H_{lw/xw}$), $\delta^2 H_{xw}$ and $\delta^2 H_{precip}$ ($\epsilon^2 H_{xw/precip}$), $\delta^2 H_{wax}$ and $\delta^2 H_{xw}$ ($\epsilon^2 H_{wax/xw}$) $\delta^2 H_{wax}$ and $\delta^2 H_{lw}$ ($\epsilon^2 H_{wax/lw}$) were also calculated using the above equation with the respective water sources.

3. Results

3.1 Concentration of n-alkanes

The *n*-alkane distributions and abundances were different for each of the 12 species analyzed from the Falkland Islands (Fig. 2, Table S1). Each of the species exhibits a strong odd over even chain length predominance (Fig. 2). Total concentration of *n*-alkanes of the 11 plant species ranges from 5.4 μ g g⁻¹ dry leaf (*B. penna-marina*) to 2321.6 μ g g⁻¹ dry leaf (*E. rubrum*) with a mean and standard deviation (1 σ) of 378.9 \pm 715.9 μ g g⁻¹ dry leaf (n = 25). For the sampled lichen species, *Usnea sp.*, the total concentration of *n*-alkanes (0.52 \pm 0.02 μ g g⁻¹ dry leaf, 1 σ , n = 2) is lower than any of the plant species. Total concentration of the *n*-alkanes of the surface lake sediment samples from Tarn 2 and Tarn 4 are 37.3

 \pm 6.8 µg g⁻¹ dry sediment (1 σ , n = 2) and 42.8 \pm 3.5 µg g⁻¹ dry sediment (1 σ , n = 3), respectively, or about one order of magnitude smaller than the plant wax concentrations found in the plant species. Chain length distribution of the *n*-alkanes varies between each of the plant growth forms and species collected (Fig. 2) with an ACL of all plant species of 28.8 \pm 1.2 (1 σ , n = 25), which ranges from 27.1 (*M. grandiflorum*) to 31.2 (*B. gummifera*). The ACL observed in the Tarn 2 and Tarn 4 is captured within the range observed in the plant species, 29.5 \pm 0.04 (1 σ , n = 2), and 29.6 \pm 0.04 (1 σ , n = 3), respectively.

3.2 Carbon isotopes of plant wax n-alkanes

The n-C₂₇, n-C₂₉, n-C₃₁ and n-C₃₃ alkanes have similar δ^{13} C_{wax} ranges (Fig 3; Table S1). Overall, B. magellanicum, a fern, exhibits the most 13 C-enriched δ^{13} C_{wax} of all the plant species for n-C₂₇, n-C₂₉, n-C₃₁. For C₃₃, the most 13 C-enriched δ^{13} C_{wax} is observed in woody shrub, E. rubrum. The most 13 C-depleted δ^{13} C_{wax} is observed in the forbs and graminoids for n-C₂₇, n-C₂₉, n-C₃₁ and n-C₃₃ (Fig 4a). Variation in δ^{13} C_{wax} for each plant species that was sampled at two or more study sites is 4.5% or less for each chain length with greatest variation with in one species, B. gummifera collected at sites 1, 3 and 4. For surface lake sediments from both Tarn 2 and Tarn 4, the n-C₂₇, n-C₂₉, n-C₃₁, and n-C₃₃ n-alkane δ^{13} C_{wax} is within the range of δ^{13} C_{wax} measured in the plant species (Fig. 4, Table S1). Comparisons of the sediment δ^{13} C_{wax} and plant δ^{13} C_{wax} may indicate which plant growth types are contributing the greatest amounts to lake sediments on the Falkland Islands. When compared to each of the plant growth forms, the sediment n-C₂₇, n-C₂₉, n-C₃₁ and n-C₃₃ δ^{13} C_{wax} is significantly different from the forbs (t-test, p < 0.0001 for n-C₂₇; p = 0.0024 for n-C₂₉; p = 0.0028 for n-C₃₁; p = 0.0073 for n-C₃₃). The sediment δ^{13} C_{wax} is also significantly different from the graminoids for n-C₂₇ (t-test, p = 0.0417), C₃₁ (t-test, p = 0.0104), and n-C₃₃ (t-test, p = 0.0124) For the other carbon chain lengths and plant growth forms the sediment δ^{13} C_{wax} is not significantly different (t-test, p > 0.05).

3.3 Hydrogen isotopes of plant wax n-alkanes

The n-C₂₇, n-C₂₉, n-C₃₁, and n-C₃₃ alkane $\delta^2 H_{wax}$ range becomes more 2H -enriched with an increase in carbon chain length (Fig. 3, 4a). Of the plant growth forms analyzed, the most 2H -enriched alkane $\delta^2 H_{wax}$ is observed in the studied ferns (B. penna-marina, B. masellanicum), for n-C₂₇, n-C₂₉, n-C₃₁, and n-C₃₃ (Fig. 4b). The most 2H -depleted alkane $\delta^2 H_{wax}$ is observed in the graminoids (C. pilosa, M. grandiflorum) for each of the four discussed carbon chain lengths (Fig. 4b). Comparisons of n-C₂₉ alkane $\delta^2 H_{wax}$ of the same species collected at different sites indicates that some species $C_{29} \delta^2 H_{wax}$ vary by site (e.g., B. gummifera: $-158 \pm 14\%$, 1σ , n = 3), whereas others did not (e.g., E. rubrum: $-176 \pm 1\%$, 1σ , n = 3). Tarn 2 and Tarn 4 surface lake sediment have a n-C₂₇, n-C₂₉, n-C₃₁ and n-C₃₃ alkane $\delta^2 H_{wax}$ that is captured in the range of the plant species analyzed. When compared to the different growth forms, the sediment $\delta^2 H_{wax}$ is significantly different from the ferns for each of the carbon chain lengths (t-test: n-C₂₇, p = 0.001; n-C₂₉, p = 0.0054; n-C₃₁, p < 0.0001; n-C₃₃, p = 0.0007). The sediment $\delta^2 H_{wax}$ is significantly different from the forbs for n-C₂₉ (t-test, p = 0.003) and n-C₃₁ (t-test, p = 0.0004), the graminoids for n-C₂₇ (t-test, p = 0.016) and the wood shrubs for n-C₃₁ (t-test, p = 0.0033).

3.4 Water hydrogen and oxygen isotopes of plant, surface waters, and precipitation

 $\delta^2 H_{lw}$ and $\delta^{18} O_{lw}$ was measured for all species except for *E. rubrum* and the lichen (Table S2). $\delta^2 H_{lw}$ has a mean of $49 \pm 16\%$ (1σ , n = 11) and $\delta^{18} O_{lw}$ has a mean of $-4.6 \pm 2.6\%$ (1σ , n = 10) (Fig. 5) for all measured species. $\delta^2 H_{xw}$ of the two species were analyzed, *B. magellanica* and *E. rubrum*, have a $\delta^2 H_{xw}$ mean of -79% (n = 1) and $-42 \pm 12\%$ (1σ , n = 3), respectively. $\delta^{18} O_{xw}$ of *B. magellanica* and *E. rubrum*, have a mean of $-6.4 \pm 0.3\%$ (1σ , n = 2) and $-2.6 \pm 4.6\%$ (1σ , n = 3), respectively. The average $\delta^2 H_{lake}$ and $\delta^{18} O_{lake}$ for the Black Tarn, Tarn 2 and Tarn 4 is $-44 \pm 3\%$ (1σ , n = 3) and $-7 \pm 1\%$ (1σ , n = 3), respectively (Fig. 5, Table 1). The low pond, located 3.1 km north of and 220 m

lower in elevation than the Black Tarn, has a more $^2\text{H-}$ and $^{18}\text{O-}$ enriched $\delta^2\text{H}_{lake}$ and $\delta^{18}\text{O}_{lake}$ than the other, higher-elevation lakes (Fig. 5). One river sample collected 1.3 km southeast of and at about the same elevation as the low pond has a $\delta^2\text{H}$ and $\delta^{18}\text{O}$ of –47% and –6.8% respectively. The local meteoric water line (LMWL) was determined using the observed precipitation at Stanley (IAEA/WMO, 2020).

Annual precipitation $\delta^2 H_{precip}$ and $\delta^{18} O_{precip}$ observed at Stanley is $-57 \pm 13\%$ (1σ , n = 92) and $-8.0 \pm 1.7\%$ (1σ , n = 92), respectively. These values are more 2H - and ^{18}O -enriched than the modelled annual precipitation from the OIPC from the location of Tarn 2, $-67 \pm 15\%$ (1σ , n = 12) for $\delta^2 H_{precip}$ and $-9.3 \pm 2.0\%$ (1σ , n = 12) for $\delta^{18}O_{precip}$ (Fig. 5) (Bowen and Revenaugh, 2003; Bowen, 2021; IAEA/WMO, 2021). For comparison, we calculated the OIPC values for each of the study sites, and due to the close proximity of the sites, the values are identical (Bowen and Revenaugh, 2003; Bowen, 2021; IAEA/WMO, 2021). Monthly precipitation isotopes observed at Stanley and modelled from the OIPC at the study locations on the Falkland Islands exhibit a seasonal cycle of $\delta^2 H_{precip}$ and $\delta^{18}O_{precip}$ of more $^2 H$ -enriched and ^{18}O -enriched precipitation during the winter (December, January and February; DJF) and more $^2 H$ -depleted and ^{18}O -depleted precipitation in the summer (June, July, August; JJA) (Fig. 1b). A stronger seasonal cycle is seen in the modelled precipitation than in the observed precipitation (Fig. 1b, 5) (Bowen and Revenaugh, 2003; Bowen, 2021; IAEA/WMO, 2021), which is due to the OIPC considering elevation, and the inland location of the sampling sites whereas Stanley is located on the coast close to sea level (~8 msl) (Bowen and Revenaugh, 2003; Bowen, 2021; IAEA/WMO, 2021). We therefore used the OIPC modelled precipitation isotopes to calculate fractionation.

3.5 Fractionation between n-alkanes and source water

One species, *B. magellanica*, in which both xylem and leaf water were measured, has a $\varepsilon^2 H_{\text{lw/xw}}$ of 39‰ (n = 1) (Table S2). For *B. magellanica* and *E. rubrum*, $\varepsilon^2 H_{\text{xw/precip}}$ is $26 \pm 13\%$ (1σ , n = 3) and – $11 \pm 3\%$ (1σ , n = 2), respectively (Table S2). Biosynthetic fractionation ($\varepsilon^2 H_{\text{wax/lw}}$) between leaf water and

each carbon chain length *n*-alkane for each species can be found in Table S2. Overall, the ferns sampled have the smallest biosynthetic fractionation for each of the four *n*-alkane carbon chain lengths whereas, one graminoid, *M. grandiflorum*, has the largest biosynthetic fractions for each of the *n*-alkane carbon chain lengths of all of the plant species (Table S2).

 $\varepsilon^2 H_{\text{wax/precip}}$ between each n-alkane carbon chain lengths were calculated using mean annual precipitation $\delta^2 H$ using the modelled precipitation isotopes from the OIPC (Bowen and Revenaugh, 2003; Bowen, 2021; IAEA/WMO, 2021). Individual plant species $\varepsilon^2 H_{\text{wax/precip}}$ for each n-alkane carbon chain length can be found in Table S2. The smallest and largest $\varepsilon^2 H_{\text{wax/precip}}$ is observed in the studied ferns and graminoids, respectively, for each n-alkane carbon chain length (Fig. 6). $\varepsilon^2 H_{\text{wax/precip}}$ is similar for both Tarn 2 and Tarn 4 (t-test, p > 0.05) and falls within range of the measured plant species (Table S2). In comparison to the plant growth forms studied here, the sediment $\varepsilon^2 H_{\text{wax/precip}}$ is significantly different from the ferns for n-C₂₇, n-C₂₉, n-C₃₁, and n-C₃₃ (t-test, p < 0.005 for each carbon chain length). The sediment $\varepsilon^2 H_{\text{wax/precip}}$ is also significantly different from the studied graminoids for C₂₇ (t-test, p = 0.02), the forbs for C₂₉ (t-test, p = 0.0231) and C₃₁ (t-test, p = 0.0004) and the woody shrubs for C₃₁ (t-test, p = 0.0016).

4. Discussion

4.1 Plant wax concentrations

Exploring how modern plants behave molecularly and isotopically in the Falkland Islands is required for paleoclimate reconstructions using plant waxes in this region. Plant wax abundance and ACL can be used to infer changes in vegetation type and environment through time (Feakins et al., 2005; Balascio et al., 2018; Schartman et al., 2020). Modern plant studies find that certain plant groups have evolved to produce different chains lengths depending on climatic (e.g. temperature, humidity and precipitation amount) and physiological (e.g. C₄ vs. C₃ plants) parameters (Schefuß et al., 2003; Sachse et

al., 2006; Hoffmann et al., 2013; Tipple and Pagani, 2013; Badewien et al., 2015; Andrae et al., 2020; Diefendorf et al., 2021). For example, previous studies have examined the relationship between midchained *n*-alkanes (C₂₃ and C₂₅) and aquatic mosses, and between longer chained *n*-alkanes (C₂₇, C₂₉, C₃₁) and woody plants and grasses (Sachse et al., 2012; Bush and McInerney, 2013; Thomas et al., 2016; Freimuth et al., 2017; Berke et al., 2019). The plants studied here have plant wax distributions similar to what is expected of known terrestrial plants with longer chain lengths (n-C₂₇ - n-C₃₃) dominating the distributions (Fig. 2) (Sachse et al., 2012; Berke et al., 2019; Andrae et al., 2020; Dion-Kirschner et al., 2020). Plant wax distributions among the Falkland Islands' plants vary among species. For example, B. magellanicum and B. magellanic have n-C₂₇ alkane as the dominant chain length, whereas in other species, such as E. rubrum and C. pilosa, n-C₂₉ alkane is the dominant chain length. Plant wax concentrations also vary on the scale of different orders of magnitude, with species such as the woody shrub, E. rubrum, having n-C₂₉ alkane concentrations close to 900 μ g g⁻¹ dry leaf, whereas other species such as the fern, B. magellanica, having n- C_{29} alkane concentrations less than 10 μ g g⁻¹ dry leaf. Similar magnitudes of *n*-alkane concentrations of woody shrubs are observed at high-latitude study sites, such as western Greenland, where Empetrum hermaphroditum has a n-C₂₉ alkane concentrations of about 600 μg g dry leaf⁻¹ (Berke et al., 2019). Slightly smaller n- C_{29} n-alkane concentrations are observed in woody shrubs in northern mid-latitudes of about 130 µg g dry leaf⁻¹ (Freimuth et al., 2017). When compared to high latitudes, the Falklands graminoid C. pilosa, has a similar concentration magnitude to other graminoids in western Greenland and other C₃ grasses in the northern mid-latitudes (Freimuth et al., 2017; Berke et al., 2019). Comparison of Falkland Island *n*-alkane concentrations to other similar modern plants of the same growth form from other regions indicate that the plants studied on the Falkland Islands produce similar concentrations of plant waxes.

375

353

354

355

356

357

358

359

360

361

362

363

364

365

366

367

368

369

370

371

372

373

374

4.2 Plant wax isotopes

377

Plant *n*-alkane $\delta^{13}C_{\text{wax}}$ and $\delta^{2}H_{\text{wax}}$, like plant wax concentrations and distributions, are sensitive to vegetation and climate changes (Sachse et al., 2012; Diefendorf and Freimuth, 2017), For example, paleoclimate records of *n*-alkane $\delta^{13}C_{\text{wax}}$ are often used to determine shifts between C_3 and C_4 plants through time (Badewien et al., 2015; Andrae et al., 2020). All of the plants studied on the Falkland Islands are C_3 plants with *n*-alkane $\delta^{13}C_{\text{wax}}$ falling into the expected range of C_3 plants, between -35 and -20% (Fig. 3, Fig. 4a) (Diefendorf and Freimuth, 2017). For $\delta^2 H_{wax}$, differences in plant type morphology or growth form have been linked to differences in $\delta^2 H_{\text{wax}}$ (Smith and Freeman, 2006; Sachse et al., 2012). On the Falkland Islands we find similar results, with each plant growth form being significantly different from the others (ANOVA, p < 0.05 for all chain lengths). The $\delta^2 H_{\text{wax}}$ observed for each of the growth forms studied here are within the range of $\delta^2 H_{wax}$ observed in other terrestrial plants found in the mid and high latitudes (Sachse et al., 2012; Freimuth et al., 2017; Berke et al., 2019; He et al., 2020). On the Falkland Islands, we observe similar trends in graminoids and ferns to other regions, with graminoids being more ²H-depleted and ferns being more ²H-enriched than other plant growth forms (Fig. 5b) (Sachse et al., 2012; Daniels et al., 2017; Berke et al., 2019; He et al., 2020). Differences in *n*-alkane $\delta^{13}C_{wax}$ and $\delta^{2}H_{wax}$ between and within plant growth forms found on the Falkland Islands can be furthered used to assess which species are contributing the greatest amounts of plant waxes to sediment archives (see Section 4.4).

395

396

394

378

379

380

381

382

383

384

385

386

387

388

389

390

391

392

393

4.3 Fractionation

397

398

399

400

401

402

Examining and quantifying the relationship between $\delta^2 H_{precip}$ and plant $\delta^2 H_{wax}$ is required to generate records of hydroclimate on the Falkland Islands. $\epsilon^2 H_{wax/precip}$ varies spatially among different terrestrial plants species and at different latitudes (Liu et al., 2006; Sachse et al., 2012; Liu and An, 2019). For example, some plants from high latitudes are found to have smaller $\epsilon^2 H_{wax/precip}$ than those at mid- and low- latitudes (Porter et al., 2016; Daniels et al., 2017; Berke et al., 2019; Dion-Kirschner et al., 2020). To

our knowledge, this study provides the first $\varepsilon^2 H_{\text{wax/precip}}$ between $\delta^2 H_{\text{wax}}$ of individual plants and $\delta^2 H_{\text{precip}}$ from the mid-latitudes in the Southern Hemisphere (Liu and An, 2019). The average $\varepsilon^2 H_{29/\text{precip}}$ of the samples collected on the Falkland Islands is $-112 \pm 16\%$ (1 σ , n = 22) (Fig. 6), which is well within the uncertainty of the global average $\varepsilon^2 H_{29/\text{precip}}$ of all plants $-121 \pm 32\%$ (n = 316) (Sachse et al., 2012), and of the updated global average $\varepsilon^2 H_{29/\text{precip}}$ of higher plants, $-116 \pm 5\%$ (n = 941) (Liu and An, 2019). This indicates that despite living in the isolated ecosystems of the Falkland Islands, variations in factors including plant wax formation, source water, rooting depth between plants is averaged out when calculating $\varepsilon_{29/\text{precip}}$ for all plants on the Falkland Islands. The $\varepsilon^2 H_{29/\text{precip}}$ of Falkland Island plants is similar to northern mid-latitude sites which have an average $\varepsilon^2 H_{29/\text{precip}}$ of -117% (n = 543) (Liu and An, 2019). The average $\varepsilon^2 H_{27/precip}$, $\varepsilon^2 H_{31/precip}$, and $\varepsilon^2 H_{33/precip}$ of the 11 plants species on the Falkland Islands is $-113 \pm 27\%$ (1 σ , n = 22), and $-103 \pm 21\%$ (1 σ , n = 18), $-99 \pm 25\%$ (1 σ , n = 8) respectively. The $\varepsilon^2 H_{\text{was/precip}}$ determined for the species on the Falkland Islands also are similar to $\varepsilon^2 H_{\text{wax/precip}}$ determined for species with similar growth forms in other regions (Sachse et al., 2012; Daniels et al., 2017; Freimuth et al., 2017). We find significant differences between each of the plant species for $\varepsilon^2 H_{27/precip}$, $\varepsilon^2 H_{29/precip}$, $\varepsilon^2 H_{31/precip}$, (oneway ANOVA, p < 0.05) but not for $\varepsilon^2 H_{33/precip}$ (oneway ANOVA, p > 0.05,) indicating that for n- C_{27} , n- C_{29} and n- C_{31} , differences in $\varepsilon^2 H_{\text{wax/precip}}$ between plant species may affect the reconstructed 2 H_{precip} using δ^{2} H_{wax} if vegetation changed through time. Variability between plants species may be attributed to differences in the biosynthesis linked to differences in plant morphology or plant growth form.

403

404

405

406

407

408

409

410

411

412

413

414

415

416

417

418

419

420

421

422

423

424

425

426

427

Biosynthetic fractionation ($\varepsilon^2 H_{wax/lw}$), exists due to biochemical reactions occurring during the synthesis of leaf waxes by plants and can vary among plants due to differences in the biosynthetic pathway of the synthesis of leaf waxes (e.g. Sachse et al., 2012). In the Falkland Islands, the average $\varepsilon^2 H_{wax/lw}$ of each of the chain lengths, n-C₂₇ ($-121 \pm 35\%$), n-C₂₉ ($-117 \pm 27\%$), n-C₃₁ ($-108 \pm 30\%$), n-C₃₃ ($-105\% \pm 30\%$), are similar to reported $\varepsilon^2 H_{wax/lw}$ from high latitudes (e.g., -120% for all chain lengths, Berke et al., 2019), but are more positive than northern mid-latitude sites (e.g., -164% for all

chain lengths; McInerney et al., 2011). The variation observed between plants species in the Falklands is likely linked to isotopic exchange and portioning of pools of water during leaf wax synthesis (Post-Beittenmiller, 1996; Sessions et al., 1999; Sachse et al., 2012). Differences in $\varepsilon^2 H_{wax/lw}$ between plant species can create complications when interpreting paleoclimate reconstructions using $\delta^2 H_{wax}$; changes observed in sediment records of $\delta^2 H_{wax}$ through time may be due to shifts in $\varepsilon^2 H_{wax/lw}$ due to changes in plant community abundances on the landscape rather than changes in $\delta^2 H_{precip}$. However, assessing concentration changes of each plant wax chain length and $\delta^{13} C_{wax}$ through time can help assess whether changes in $\varepsilon^2 H_{wax/lw}$ are linked to changes in plant community and should be considered when interpreting climate records in the Falkland Islands. Similarly, independent proxies (e.g. pollen, sedimentary ancient DNA) from sediment archives can help constrain changes in plant contribution to sediments through time (Fréchette and de Vernal, 2009; Feakins, 2013; Crump et al., 2019).

4.4 Contribution of plant waxes to sediment archives

Plant wax concentration and distribution, $\delta^{13}C_{wax}$ and δ^2H_{wax} of both the modern plants and modern lake surface sediments can provide additional guidance for interpreting records of past climate and vegetation by assessing what plants are contributing the most to sediment archives. In the surface lake sediments from Tarn 2 and Tarn 4, n- C_{29} alkane is the most concentrated chain length followed by the n- C_{31} alkane. The plant wax chain length distribution for each of these lakes is not identical to any of the studied plant species, indicating that the sediment is a mixture of some of all the plants found in the watersheds. The greatest total concentration of plant waxes are observed in the forb B. gummifera, and in the woody shrub, E. rubrum, suggesting that if each plant is sourced equally, a significant amount of plant waxes found in sediment archives would be from these two species (Fig. 2). The $\delta^{13}C_{wax}$ and δ^2H_{wax} of E. rubrum is similar to the sediment samples for n- C_{27} , n- C_{29} , n- C_{31} and n- C_{33} , (t-test, p > 0.05 for $\delta^{13}C_{wax}$ and δ^2H_{wax}), whereas the $\delta^{13}C_{wax}$ of B. gummifera is different from the surface sediment for n- C_{27} , n- C_{29} , n-

n-C₃₁ (t-test, p < 0.0034), and the δ^2 H_{wax} of B. gummifera is different from the surface sediment for n-C₂₉, and n-C₃₁ (t-test, p < 0.0015) (Fig. 3). This suggests that because E. rubrum is similar to the sediment samples, it may be contributing more to the sediment than B. gummifera despite both having large concentrations of plant waxes. The $\delta^{13}C_{\text{wax}}$ of the n- C_{27} , n- C_{29} , and n- C_{31} in the sediment samples is more ¹³C-enriched than all of the plant growth forms except the fern (Fig. 5a). This indicates that ferns, in particular, B. magellanicum, are contributing to plant waxes found in the sediment (Fig. 4a, b, and c). B. magellanicum does not produce high concentrations of n- C_{33} (Fig. 2), so the n- C_{33} found in the sediment archives is likely from other plants. A similar pattern is found in the $\delta^2 H_{wax}$ of the n- C_{27} , n- C_{29} , n- C_{31} and n-C₃₃ in the sediment samples and the graminoids, where the sediment is 2 H-depleted relative to all of the growth forms besides the graminoids (Fig. 5b). This suggests that one or both the graminoids studied on the Falkland Islands is a primary contributor to the waxes found in the sediment. The graminoid, M. grandiflorum, has low concentrations ($<15 \mu g g^{-1}$ dry leaf) (Fig. 2) indicating that this species is likely contributing smaller amounts to the sediment archives than the other graminoid, C. pilosa, which has higher concentrations of waxes (Fig. 2). The forbs, which have a similar $\delta^{13}C_{wax}$ and $\delta^{2}H_{wax}$ to the sediment wax samples (see Section 3.3), in addition to E. rubrum, B. magellanicum and C. pilosa, are likely contributing the most waxes to sediment archives. E. rubrum and C. pilosa are the most common plants found on the Falkland Islands and are present throughout the field area, confirming that the waxes of these two species are likely contributing to the sediment waxes.

453

454

455

456

457

458

459

460

461

462

463

464

465

466

467

468

469

470

471

472

473

474

475

476

477

There can be limitations with applying molecular and isotopic data from modern plants to sediment archives, because this can assume that waxes from each plant are sourced equally. However, this is often not the case with different plant types and species being preferentially transported and deposited into the lake due to proximity and taphonomic controls (e.g., Freimuth et al., 2019). In the Falkland Islands, plant waxes are likely deposited into sediment via numerous processes including wind ablation from leaf surfaces, remobilization of waxes from soils and from leaves transported to the lake via wind (Diefendorf and Freimuth, 2017; Freimuth et al., 2021). The first process, wind ablation of waxes from

leaf surfaces, occurs when waxes are transported via aerosol and then are deposited into lakes by wet deposition from precipitation (Gao et al., 2014; Nelson et al., 2018). If waxes are scrubbed from aerosols via snowfall on the Falkland Islands, waxes could be deposited into the lake during the spring melt period when the snow in the surrounding catchment melts. However, aerosol n-alkane concentrations have been observed to be greatest during spring when leaves emerge (Nelson et al., 2017), indicating that there may not be much deposition via this mechanism in winter. Future collection of aerosols would indicate the plant wax concentration and isotopes that are deposited via this mechanism into lake sediment. The second process, deposition via remobilization of soils into the lake, depends on certain lake-specific parameters, including lake catchment, size and hydrology, landscape erosion, and soil development (Douglas et al., 2014; Gierga et al., 2016). The studied lakes are circues with steep slopes suggesting that soil erosion into the lake is a likely method of deposition of waxes in the Falkland lakes. The third mechanism, direct deposition of leaves into lakes, may result in certain plant species' waxes to dominate the lake sediment due to taphonomic differences between leaves may result in sediment waxes being dominated by certain plant species (Diefendorf and Freimuth, 2017). For example, lighter and smaller leaves typically travel further than larger and heavier leaves (Spicer, 1981; Spicer and Wolfe, 1987). Woody vegetation surrounding the lake catchment tends to dominate the leaves, and therefore the waxes, entering the lake (Drake and Burrows, 1980; Diefendorf and Freimuth, 2017; Freimuth et al., 2019). This suggests that on the Falkland Islands, E. rubrum, a woody shrub, may contribute more waxes to the sediment than other non-woody plants on the landscape. Our results indicate that sediment $\delta^{13}C_{wax}$ and $\delta^2 H_{\text{wax}}$ is similar to the $\delta^{13} C_{\text{wax}}$ and $\delta^2 H_{\text{wax}}$ of E. rubrum (see last paragraph), suggesting that this taphonomic bias could exist on the Falkland Islands. However, there has been little work done studying plant wax transport and taphonomic processes in landscapes such as the Falkland Islands where the vegetation is dominated by low-stature plants including herbs and shrubs. Taphonomic biases that results in a few species dominating the plant wax contributions to lake sediment archives is important to consider when reconstructing past climates using $\delta^2 H_{wax}$.

478

479

480

481

482

483

484

485

486

487

488

489

490

491

492

493

494

495

496

497

498

499

500

501

505

506

507

508

509

510

511

512

513

514

515

516

517

518

519

520

521

522

523

524

525

526

527

503

504

Next, we establish how meteoric water (i.e. precipitation, lake water) varies isotopically on the Falkland Islands, how that may affect plant $\delta^2 H_{wax}$ values, and what that implies for paleoclimate reconstructions. The isotopic composition of meteoric waters can vary both regionally and seasonally due to differences in moisture source location, moisture source distance and evaporation (Dansgaard, 1964; Gat, 1996; Bowen et al., 2019). Based on global meteoric waters observations, we expect precipitation isotopes observed on the Falkland Islands to vary geographically by distance inland from the ocean (e.g. coastal vs. inland) and by the elevation of the site. Similarly, we expect precipitation isotopes to vary seasonally on the Falkland Islands as a result of the seasonal changes in moisture sources location observed in the Falkland Islands (Groff et al., 2020). Observed long term (n = 15 years) precipitation isotopes from Stanley and modelled precipitation isotopes from OIPC do exhibit this seasonal trend of ²H-depleted precipitation in austral winter (June, July, August; JJA) (Fig. 1a, b) and more ²H-enriched precipitation in austral summer (December, January, February; DJF) (Section 3.4) (Bowen and Revenaugh, 2003; Bowen, 2021; IAEA/WMO, 2021). The seasonal variation observed in the observed $\delta^2 H_{\text{precip}}$ at Stanley Bay and modelled $\delta^2 H_{\text{precip}}$ at the study sites is likely due to changes in moisture source. A greater amount of precipitation during JJA comes from the south, where source water, circulation patterns, temperatures, and distance travelled results in precipitation that is ²H-depleted relative to precipitation that comes from the north, (Groff et al., 2020; Spoth, 2020). Understanding how $\delta^2 H_{\text{precip}}$ varies in the Falkland Islands has implications for terrestrial plants that utilize this precipitation to synthesize plant waxes and how they should be interpreted in sediment archives.

Precipitation isotopes along with climatic parameters (e.g. timing of snowmelt), and proxy mechanisms (e.g. timing of leaf wax synthesis) influence terrestrial plant $\delta^2 H_{wax}$ preserved in lake sediment archives (Tipple et al., 2013; Freimuth et al., 2017; Thomas et al., 2020). For example, plants

that synthesize terrestrial leaf waxes at certain times of the year in regions where is a seasonal cycle of $\delta^2 H_{\text{precip}}$, including the sites in this study, may be seasonally biased to the $\delta^2 H_{\text{precip}}$ at the time of synthesis. Similar to some high latitude sites in the Arctic, the high elevation on the Falkland Islands experiences snow cover during winter. Depending on the amount of snow that falls and persists on the landscape, terrestrial plants may utilize soil water that is primarily made of snowmelt during wax synthesis in the spring. In this case, terrestrial plant $\delta^2 H_{wax}$ would be biased towards winter $\delta^2 H_{precip}$. However, if the plant waxes are made throughout the entire growing season (i.e. spring, summer), or there was little snowmelt on a given year, $\delta^2 H_{\text{wax}}$ may be biased towards annual $\delta^2 H_{\text{precip}}$ or summer $\delta^2 H_{\text{precip}}$ because the plants are using a combination of winter snowmelt and summer precipitation or just summer precipitation to synthesis their waxes. In the Falkland Islands, based on the modelled precipitation isotopes from the OIPC, average spring and summer (SONDJF) $\delta^2 H_{\text{precip}}$ is $-61 \pm 16\%$ (1σ , n = 6) and mean annual $\delta^2 H_{\text{precip}}$ is $-67 \pm 15\%$ (1σ , n = 12). This means that because these values are similar, regardless of whether the plants are only using spring and summer precipitation or some combination of winter snowmelt and spring and summer precipitation, terrestrial plant $\delta^2 H_{wax}$ mean annual precipitation. The same conclusion can be made based on the observed precipitation at Stanley (IAEA, 2021). This indicates that sediment records of terrestrial plant $\delta^2 H_{\text{wax}}$ can be used to reconstruct mean annual $\delta^2 H_{\text{precip}}$.

The relationship between plant $\delta^2 H_{xw}$ and $\delta^2 H_{precip}(\epsilon^2 H_{xw/precip})$ can be used to characterize the amount of soil evaporation occurring in the local environment (Feakins and Sessions, 2010), an important factor to consider when interpreting terrestrial plant $\delta^2 H_{wax}$ records. When plants uptake water by the roots, there is no fractionation (with the exception of salt water tolerance plants), so any variation between plant $\delta^2 H_{xw}$ and $\delta^2 H_{precip}$ is due to soil evaporation (Ehleringer et al., 1991; Ehleringer and Dawson, 1992; Schwendenmann et al., 2015; Cernusak et al., 2016; Sprenger et al., 2016). Increased soil water evaporation would cause the plant source water to become 2H -enriched relative to the $\delta^2 H_{precip}$ resulting in a larger $\epsilon^2 H_{xw/precip}$. The two plant species in this study analyzed for $\delta^2 H_{xw}$, B. magellanic and E. rubrum, have a $\epsilon^2 H_{xw/precip}$ of $-17 \pm 3\%$ (1σ , n = 2) and $18 \pm 15\%$ (1σ , n = 3), respectively. The difference in

 $\varepsilon^2 H_{xw/precip}$ between the two species may be a result of each plants species utilizing pools of soil water from different depths within the soil (Ehleringer et al., 1991; Williams and Ehleringer, 2000) or due to the timing of sampling during the year. The $\varepsilon^2 H_{xw/precip}$ of the two sampled plants here are similar than those observed at high latitudes, such as western Greenland (14 ± 17‰, 1 σ , n = 23; Berke et al., 2019) and Alaska (26 ± 17‰, 1 σ , n = 24; O'Connor et al., 2020). Overall, the $\varepsilon^2 H_{xw/precip}$ of the two sampled plants on the Falkland Islands indicate that there is minimum soil evaporation occurring, further supporting that terrestrial plant $\delta^2 H_{wax}$ reflects mean annual precipitation without much influence of evaporation.

553

554

555

556

557

558

559

560

561

562

563

564

565

566

567

568

569

570

571

572

573

574

575

576

577

Examining modern $\delta^2 H_{lake}$ can aid in interpreting records using aquatic plant $\delta^2 H_{wax}$. Aquatic plants utilize lake water to synthesize their waxes, so aquatic plant $\delta^2 H_{wax}$ reflects $\delta^2 H_{lake}$ is function of both the $\delta^2 H_{precip}$ of the precipitation falling into the lake and surrounding catchment and any evaporation occurring in the lake basin (Gat, 1996; Anderson et al., 2016; Cluett and Thomas, 2020). Lake water $\delta^2 H$ may be seasonally biased depending on whether $\delta^2 H_{\text{precip}}$ varies seasonally and whether lake-water residence times, or the time it takes for the lake water to completely flush, is short enough for water in the lake to completely turnover (< 3 months) (Anderson et al., 2016; Thomas et al., 2020). Based on the modelled and observed $\delta^2 H_{\text{precip}}$ and on the observation that lake water isotopes reflect precipitation isotopes falling into the lake and surrounding catchments, we expect that the lake water from the tarns to reflect precipitation isotopes with some seasonal variation with possible evaporative effects. Average summer $\delta^2 H_{lake}$ collected from the Black Tarn, Tarn 2 and Tarn 4 (-44 ± 3‰, 1 σ , n = 5) is similar to observed ($-48 \pm 10\%$, 1σ , n = 23) and modelled summer precipitation ($-48 \pm 7\%$, 1σ , n = 3) (Fig. 1b) for DJF indicating that lake water reflects precipitation isotopes in the Falkland Islands during the summer (the time of lake water collection). Lake water δ^2H from the Black Tarn, Tarn 2 and Tarn 4 fall on the LMWL (Fig. 3), suggesting that there is minimal lake water evaporation under today's climate. Average relative humidity on the Falkland Islands is 83%, with mist being common in the cirques suggesting that there is little evaporation, especially in regions of high elevation over the study lakes. Persistent winds on the Falkland Islands may result in increased evaporation. However, because the lake water $\delta^2 H$ falls on

the LWML, there was likely minimal lake water evaporation at the time of the sample collection. Sample collection occurred during the summer, when temperatures are close to their maximum, and evaporation would have been at its greatest, suggesting that there is little lake water evaporation occurring in the study lakes year-round. One lake water sample from the small pond, located at low elevation plots below and to the right of the LMWL indicating that this pond has some evaporative enrichment compared to the other lakes. There is likely due to lower humidity and less fog that persists on this pond than at higher elevations and the fact that this pond is shallow (\sim 1 m) so there is a greater effect of evaporation on the water isotopes. Today, these results indicate the $\delta^2 H_{lake}$ currently reflects summer precipitation and aquatic proxies that reflect $\delta^2 H_{lake}$ therefore reflect summer precipitation with minimum evaporative effects.

5. Conclusion

This new dataset of meteoric waters, modern plant, and surface sediment molecular and isotopic data provides new insights for generating hydroclimate records on the Falkland Islands. Plant wax concentration, distribution, $\delta^2 H_{wax}$ and $\delta^{13} C_{wax}$ among plant growth types observed on the Falkland Island is similar to that of plants found in other mid- and high-latitude sites. Comparisons of plant wax concentration, $\delta^2 H_{wax}$, $\delta^{13} C_{wax}$ and the calculated $\epsilon^2 H_{wax/precip}$ of the sampled plants and sediment samples suggests that *E. rubrum*, *B. magellanicum* and *C. pilosa* are contributing the most to the waxes in sediment archives, in keeping with their abundance on the landscape. Mean annual $\delta^2 H_{precip}$ and spring and summer biased $\delta^2 H_{precip}$ are similar, indicating that regardless of what terrestrial plants on the Falkland Islands are synthesizing waxes, terrestrial plant $\delta^2 H_{wax}$ reflects mean annual precipitation. Therefore, sedimentary records that reconstruct terrestrial plant $\delta^2 H_{wax}$ can be interpreted as changes in mean annual $\delta^2 H_{precip}$. Lake-water samples $\delta^2 H_{lake}$ reflect summer precipitation and fall on the LMWL indicating that, at least for recent similar climate states, there is minimal surface-water evaporation in the

Falkland Islands, and for similar climates, $\delta^2 H_{lake}$ proxies can be interpreted as summer precipitation. Overall, this survey of modern plants and surfaces establishes the framework needed to interpret records of $\delta^2 H_{wax}$ from sediment archives in the Falkland Islands and other mid-latitude maritime climatic regions, allowing for reconstructions of past hydroclimate.

Acknowledgements

We would like to thank Sarah Hammer for laboratory support and MacKenzie King and Samuel Little for their assistance with sample preparation. We also thank Antony Smith of Discovery Falklands who provided key logistical support, and the staff at the South Atlantic Environmental Research Institute and the Falklands Islands Government for assistance. We also wish to thank Gill Smith and the late Colin Smith, landowners, Ken Morrison, Teresa Smith, Richard Fogerty, and the many others in the Falkland Islands who assisted us. This research was supported by the US National Science Foundation (EAR-1636740 to AFD and TVL). Sample collection was funded by the University of Maine. Acknowledgment is made to the Donors of the American Chemical Society Petroleum Research Fund for partial support of the research (PRF #60163-ND2 to AFD).

Appendix A. Supplementary data

The supplementary data and information to this article can be accessed online at (insert link to supplement here). Water isotope data will publicly available on waterisotopes.org. Falkland plant molecular and isotopic data will be uploaded to PANGAEA.

References

628

629 Anderson, L., Berkelhammer, M., Barron, J.A., Steinman, B.A., Finney, B.P., Abbott, M.B., 2016. Lake 630 oxygen isotopes as recorders of North American Rocky Mountain hydroclimate: Holocene 631 patterns and variability at multi-decadal to millennial time scales. Global and Planetary Change 632 137, 131-148. 633 Anderson, R.F., Ali, S., Bradtmiller, L.I., Nielsen, S.H.H., Fleisher, M.O., Anderson, B.E., Burckle, L.H., 634 2009. Wind-Driven upwelling in the Southern Ocean and the deglacial rise in atmospheric CO₂. 635 science 323, 1443-1448. 636 Andrae, J.W., McInerney, F.A., Sniderman, J.M.K., 2020. Carbon isotope systematics of leaf wax n-637 alkanes in a temperate lacustrine depositional environment. Organic Geochemistry 150, 104121. 638 Badewien, T., Vogts, A., Rullkötter, J., 2015. N-Alkane distribution and carbon stable isotope 639 composition in leaf waxes of C₃ and C₄ plants from Angola. Organic Geochemistry 89-90, 71-79. 640 Balascio, N.L., D'Andrea, W.J., Gjerde, M., Bakke, J., 2018. Hydroclimate variability of High Arctic 641 Svalbard during the Holocene inferred from hydrogen isotopes of leaf waxes. Quaternary Science Reviews 183, 177-187. 642 643 Berke, M.A., Cartagena Sierra, A., Bush, R., Cheah, D., O'Connor, K., 2019. Controls on leaf wax 644 fractionation and δ^2 H values in tundra vascular plants from western Greenland. Geochimica et Cosmochimica Acta 244, 565-583. 645 646 Bokhorst, S., Huiskes, A., Convey, P., Aerts, R., 2007. The effect of environmental change on vascular 647 plant and cryptogam communities from the Falkland Islands and the Maritime Antarctic. BMC 648 Ecology 7, 15. 649 Bowen, G.J., 2021. The online isotopes in precipitation calculator, version 3.1. Accessible at 650 http://www.waterisotopes.org. 651 Bowen, G.J., Cai, Z., Fiorella, R.P., Putman, A.L., 2019. Isotopes in the water cycle: Regional- to global-652 scale patterns and applications. Annual Review of Earth and Planetary Sciences 47, 453-479.

- Bowen, G.J., Revenaugh, J., 2003. Interpolating the isotopic composition of modern meteoric
- precipitation. Water Resources Research 39, 1299.
- Broughton, D.A., McAdam, J.H., 2002. A eed sata list for the Falkland Islands vascular flora. Oryx 36,
- 656 279-287.
- Bush, R.T., McInerney, F.A., 2013. Leaf wax *n*-alkane distributions in and across modern plants:
- Implications for paleoecology and chemotaxonomy. Geochimica et Cosmochimica Acta 117,
- 659 161-179.
- 660 Cernusak, L.A., Barbour, M.M., Arndt, S.K., Cheesman, A.W., English, N.B., Feild, T.S., Helliker, B.R.,
- Holloway-Phillips, M.M., Holtum, J.A.M., Kahmen, A., McInerney, F.A., Munksgaard, N.C.,
- 662 Simonin, K.A., Song, X., Stuart-Williams, H., West, J.B., Farquhar, G.D., 2016. Stable isotopes
- in leaf water of terrestrial plants. Plant, Cell & Environment 39, 1087-1102.
- 664 Chavaillaz, Y., Codron, F., Kageyama, M., 2013. Southern westerlies in LGM and future (RCP4.5)
- climates. Climate of the Past 9, 517-524.
- 666 Cluett, A.A., Thomas, E.K., 2020. Resolving combined influences of inflow and evaporation on western
- Greenland lake water isotopes to inform paleoclimate inferences. Journal of Paleolimnology, 251-
- 668 268.
- 669 Crump, S.E., Miller, G.H., Power, M., Sepúlveda, J., Dildar, N., Coghlan, M., Bunce, M., 2019. Arctic
- shrub colonization lagged peak postglacial warmth: Molecular evidence in lake sediment from
- Arctic Canada. Global Change Biology 25, 4244-4256.
- Daniels, W.C., Russell, J.M., Giblin, A.E., Welker, J.M., Klein, E.S., Huang, Y., 2017. Hydrogen isotope
- fractionation in leaf waxes in the Alaskan Arctic tundra. Geochimica et Cosmochimica Acta 213,
- 674 216-236.
- Dansgaard, W., 1964. Stable isotopes in precipitation. Tellus 16, 436-468.
- Diefendorf, A.F., Bickford, C.P., Schlanser, K.M., Freimuth, E.J., Hannon, J.S., Grossiord, C.,
- McDowell, N.G., 2021. Plant wax and carbon isotope response to heat and drought in the conifer
- Juniperus monosperma. Organic Geochemistry 153, 104197.

- Diefendorf, A.F., Freimuth, E.J., 2017. Extracting the most from terrestrial plant-derived *n*-alkyl lipids
- and their carbon isotopes from the sedimentary record: A review. Organic Geochemistry 103, 1-
- 681 21.
- 682 Dion-Kirschner, H., McFarlin, J.M., Masterson, A.L., Axford, Y., Osburn, M.R., 2020. Modern
- constraints on the sources and climate signals recorded by sedimentary plant waxes in west
- 684 Greenland. Geochimica et Cosmochimica Acta 286, 336-354.
- Douglas, P.M.J., Pagani, M., Eglinton, T.I., Brenner, M., Hodell, D.A., Curtis, J.H., Ma, K.F.,
- Breckenridge, A., 2014. Pre-aged plant waxes in tropical lake sediments and their influence on
- the chronology of molecular paleoclimate proxy records. Geochimica et Cosmochimica Acta 141,
- 688 346-364.
- Drake, H., Burrows, C.J., 1980. The influx of potential macrofossils into Lady Lake, north Westland,
- New Zealand. New Zealand Journal of Botany 18, 257-274.
- Duan, Y., Xu, L., 2012. Distributions of *n*-alkanes and their hydrogen isotopic composition in plants from
- Lake Qinghai (China) and the surrounding area. Applied Geochemistry 27, 806-814.
- 693 Ehleringer, J., Dawson, T., 1992. Water uptake by plants: perspectives from stable isotope composition.
- 694 Plant, cell & environment 15, 1073-1082.
- 695 Ehleringer, J.R., Phillips, S.L., William, S.F.S., Sandquist, D.R., 1991. Differential utilization of summer
- rains by desert Ppants. Oecologia 88, 430-434.
- Eley, Y., Dawson, L., Black, S., Andrews, J., Pedentchouk, N., 2014. Understanding ²H/¹H systematics of
- 698 leaf wax *n*-alkanes in coastal plants at Stiffkey saltmarsh, Norfolk, UK. Geochimica et
- 699 Cosmochimica Acta 128, 13-28.
- Feakins, S.J., 2013. Pollen-corrected leaf wax D/H reconstructions of northeast African hydrological
- changes during the late Miocene. Palaeogeography, Palaeoclimatology, Palaeoecology 374, 62-
- 702 71.
- Feakins, S.J., Bentley, L.P., Salinas, N., Shenkin, A., Blonder, B., Goldsmith, G.R., Ponton, C., Arvin,
- 704 L.J., Wu, M.S., Peters, T., West, A.J., Martin, R.E., Enquist, B.J., Asner, G.P., Malhi, Y., 2016.

705 Plant leaf wax biomarkers capture gradients in hydrogen isotopes of precipitation from the Andes 706 and Amazon. Geochimica et Cosmochimica Acta 182, 155-172. Feakins, S.J., deMenocal, P.B., Eglinton, T.I., 2005. Biomarker records of late Neogene changes in 707 708 northeast African vegetation. Geology 33, 977-980. 709 Feakins, S.J., Sessions, A.L., 2010. Controls on the D/H ratios of plant leaf waxes in an arid ecosystem. 710 Geochimica et Cosmochimica Acta 74, 2128-2141. 711 Fletcher, M.-S., Moreno, P.I., 2012. Have the Southern westerlies changed in a zonally symmetric manner 712 over the last 14,000 years? A hemisphere-wide take on a controversial problem. Quaternary 713 International 253, 32-46. 714 Fréchette, B., de Vernal, A., 2009. Relationship between Holocene climate variations over southern 715 Greenland and eastern Baffin Island and synoptic circulation pattern. Climate of the past 5, 347-716 359. 717 Freimuth, E.J., Diefendorf, A.F., Lowell, T.V., 2017. Hydrogen isotopes of *n*-alkanes and *n*-alkaneic 718 acids as tracers of precipitation in a temperate forest and implications for paleorecords. 719 Geochimica et Cosmochimica Acta 206, 166-183. 720 Freimuth, E.J., Diefendorf, A.F., Lowell, T.V., Bates, B.R., Schartman, A., Bird, B.W., Landis, J.D., 721 Stewart, A.K., 2020. Contrasting sensitivity of lake sediment *n*-alkanoic acids and *n*-alkanes to 722 basin-scale vegetation and regional-scale precipitation δ^2 H in the Adirondack Mountains, NY 723 (USA). Geochimica et Cosmochimica Acta 268, 22-41. 724 Freimuth, E.J., Diefendorf, A.F., Lowell, T.V., Schartman, A.K., Landis, J.D., Stewart, A.K., Bates, B.R., 725 2021. Centennial-scale age offsets of plant wax n-alkanes in Adirondack lake sediments. 726 Geochimica et Cosmochimica Acta. 727 Freimuth, E.J., Diefendorf, A.F., Lowell, T.V., Wiles, G.C., 2019. Sedimentary *n*-alkanes and *n*-alkanoic 728 acids in a temperate bog are biased toward woody plants. Organic Geochemistry 128, 94-107.

729 Gao, L., Zheng, M., Fraser, M., Huang, Y., 2014. Comparable hydrogen isotopic fractionation of plant 730 leaf wax n-alkanoic acids in arid and humid subtropical ecosystems. Geochemistry, Geophysics, 731 Geosystems 15, 361-373. 732 Gat, J.R., 1996. Oxygen and hydrogen isotopes in the hydrological cycle. Annual Review of Earth and 733 Planetary Sciences 24, 225-262. 734 Gierga, M., Hajdas, I., van Raden, U.J., Gilli, A., Wacker, L., Sturm, M., Bernasconi, S.M., Smittenberg, 735 R.H., 2016. Long-stored soil carbon released by prehistoric land use: Evidence from compound-736 specific radiocarbon analysis on Soppensee lake sediments. Quaternary Science Reviews 144, 737 123-131. 738 Groff, D.V., Williams, D.G., Gill, J.L., 2020. Modern calibration of Poa flabellata (tussac grass) as a new 739 paleoclimate proxy in the South Atlantic. Biogeosciences 17, 4545-4557. 740 Hall, B., Lowell, T., Brickle, P., 2020. Multiple glacial advances of similar extent at ~20-45 ka on Mt. 741 Usborne, East Falkland, South Atlantic region. Quaternary Science Reviews 250, 106677. 742 He, D., Ladd, S.N, Saunders, C.J., Mead, R.N., Jaffé, R., 2020. Distribution of *n*-alkanes and their $\delta^2 H$ and δ^{13} C values in typical plants along a terrestrial-coastal-oceanic gradient. Geochimica et 743 744 Cosmochimica Acta 281, 31-52. 745 Hoffmann, B., Kahmen, A., Cernusak, L.A., Arndt, S.K., Sachse, D., 2013. Abundance and distribution 746 of leaf wax n-alkanes in leaves of Acacia and Eucalyptus trees along a strong humidity gradient 747 in northern Australia. Organic Geochemistry 62, 62-67. 748 Hou, J., D'Andrea, W.J., MacDonald, D., Huang, Y., 2007. Hydrogen isotopic variability in leaf waxes 749 among terrestrial and aquatic plants around Blood Pond, Massachusetts (USA). Organic 750 Geochemistry 38, 977-984. 751 IAEA/WMO, 2021. Global Network of Isotopes in Precipitation. The GNIP Database. Accessible at

https://nucleus.iaea.org/wiser.

753 Kahmen, A., Hoffmann, B., Schefuss, E., Arndt, S.K., Cernusak, L.A., West, J.B., Sachse, D., 2013. Leaf 754 water deuterium enrichment shapes leaf wax *n*-alkane D values of angiosperm plants II: 755 Observational evidence and global implications, Geochimica et Cosmochimica Acta 111, 50-63. 756 Kitoh, A., Kusunoki, S., Nakaegawa, T., 2011. Climate change projections over South America in the late 757 21st century with the 20 and 60 km mesh Meteorological Research Institute atmospheric general 758 circulation model (MRI-AGCM). Journal of Geophysical Research. Atmospheres 116, D06105. 759 Lister, D.H., Jones, P.D., 2015. Long-term temperature and precipitation records from the Falkland 760 Islands. International Journal of Climatology 35, 1224-1231. 761 Liu, J., An, Z., 2019. Variations in hydrogen isotopic fractionation in higher plants and sediments across 762 different latitudes: Implications for paleohydrological reconstruction. Science of The Total 763 Environment 650, 470-478. 764 Liu, W., Yang, H., Li, L., 2006. Hydrogen isotopic compositions of *n*-alkanes from terrestrial plants 765 correlate with their ecological life forms. Oecologia 150, 330-338. 766 McFarlin, J.M., Axford, Y., Masterson, A.L., Osburn, M.R., 2019. Calibration of modern sedimentary 767 δ^2 H plant wax-water relationships in Greenland lakes. Quaternary Science Reviews 225, 105978. 768 McInerney, F.A., Helliker, B.R., Freeman, K.H., 2011. Hydrogen isotope ratios of leaf wax *n*-alkanes in 769 grasses are insensitive to transpiration. Geochimica et Cosmochimica Acta 75, 541-554. 770 Moore, D.M., 1968. The vascular flora of the Falkland Islands. The vascular flora of the Falkland Islands. 771 Nelson, D.B., Knohl, A., Sachse, D., Schefuc, E., Kahmen, A., 2017. Sources and abundances of leaf 772 waxes in aerosols in central Europe. Geochimica et Cosmochimica Acta 198, 299-314. 773 Nelson, D.B., Ladd, S.N., Schubert, C.J., Kahmen, A., 2018. Rapid atmospheric transport and large-scale 774 deposition of recently synthesized plant waxes. Geochimica et Cosmochimica Acta 222, 599-617. NOAA, 2021. National Climatic Data Center (NCDC). Global Historical Climatology Network. 775 776 Accessible at https://www.ncdc.noaa.gov. 777 O'Connor, K.F., Berke, M.A., Ziolkowski, L.A., 2020. Hydrogen isotope fractionation in modern plants

along a boreal-tundra transect in Alaska. Organic Geochemistry 147, 104064.

- Paul, D., Skrzypek, G., 2006. Flushing time and storage effects on the accuracy and precision of carbon
- and oxygen isotope ratios of sample using the Gasbench II technique. Rapid Communications in
- 781 Mass Spectrometry 20, 2033-2040.
- Polissar, P.J., D'Andrea, W.J., 2014. Uncertainty in paleohydrologic reconstructions from molecular δD
- values. Geochimica et Cosmochimica Acta 129, 146-156.
- Porter, T.J., Froese, D.G., Feakins, S.J., Bindeman, I.N., Mahony, M.E., Pautler, B.G., Reichart, G.-J.,
- Sanborn, P.T., Simpson, M.J., Weijers, J.W.H., 2016. Multiple water isotope proxy
- 786 reconstruction of extremely low last glacial temperatures in Eastern Beringia (Western Arctic).
- 787 Quaternary Science Reviews 137, 113-125.
- Post-Beittenmiller, D., 1996. Biochemistry and molecular biology of wax production in plants. Annual
- review of plant physiology and plant molecular biology 47, 405-430.
- Rach, O., Kahmen, A., Brauer, A., Sachse, D., 2017. A dual-biomarker approach for quantification of
- changes in relative humidity from sedimentary lipid D/H ratios. Clim. Past 13, 741-757.
- Rojas, M., Moreno, P., Kageyama, M., Crucifix, M., Hewitt, C., Abe-Ouchi, A., Ohgaito, R., Brady, E.C.,
- Hope, P., 2009. The Southern westerlies during the last glacial maximum in PMIP2 simulations.
- 794 Climate Dynamics 32, 525-548.
- Russell, J.L., Dixon, K.W., Gnanadesikan, A., Stouffer, R.J., Toggweiler, J.R., 2006. The Southern
- Hemisphere westerlies in a warming world: Propping open the door to the deep ocean. Journal of
- 797 Climate 19, 6382-6390.
- Sachse, D., Billault, I., Bowen, G.J., Chikaraishi, Y., Dawson, T.E., Feakins, S.J., Freeman, K.H., Magill,
- C.R., McInerney, F.A., Van der Meer, M.T.J., Polissar, P., Robins, R.J., Sachs, J.P., Schmidt, H.-
- L., Sessions, A.L., White, J.W.C., West, J.B., Kahmen, A., 2012. Molecular paleohydrology:
- Interpreting the hydrogen-isotopic composition of lipid biomarkers from photosynthesizing
- organisms. Annual Review of Earth and Planetary Sciences 40, 221-249.
- 803 Sachse, D., Radke, J., Gleixner, G., 2004. Hydrogen isotope ratios of recent lacustrine sedimentary *n*-
- alkanes record modern climate variability. Geochimica et Cosmochimica Acta 68, 4877-4889.

805	Sachse, D., Radke, J., Gleixner, G., 2006. δD values of individual n-alkanes from terrestrial plants along a
806	climatic gradient - Implications for the sedimentary biomarker record. Organic Geochemistry 37,
807	469-483.
808	Schartman, A.K., Diefendorf, A.F., Lowell, T.V., Freimuth, E.J., Stewart, A.K., Landis, J.D., Bates, B.R.,
809	2020. Stable source of Holocene spring precipitation recorded in leaf wax hydrogen-isotope ratios
810	from two New York lakes. Quaternary science reviews 240, 106357.
811	Schefuß, E., Ratmeyer, V., Stuut, JB.W., Jansen, J.H.F., Sinninghe Damsté, J.S., 2003. Carbon isotope
812	analyses of <i>n</i> -alkanes in dust from the lower atmosphere over the central eastern Atlantic.
813	Geochimica et Cosmochimica Acta 67, 1757-1767.
814	Schwendenmann, L., Pendall, E., Sanchez-Bragado, R., Kunert, N., Hölscher, D., 2015. Tree water
815	uptake in a tropical plantation varying in tree diversity: interspecific differences, seasonal shifts
816	and complementarity. Ecohydrology 8, 1-12.
817	Sessions, A.L., Burgoyne, T.W., Schimmelmann, A., Hayes, J.M., 1999. Fractionation of hydrogen
818	isotopes in lipid biosynthesis. Organic Geochemistry 30, 1193-1200.
819	Smith, F.A., Freeman, K.H., 2006. Influence of physiology and climate on δD of leaf wax <i>n</i> -alkanes from
820	C ₃ and C ₄ grasses. Geochimica et Cosmochimica Acta 70, 1172-1187.
821	Spicer, R.A., 1981. The sorting and deposition of allochthonous plant material in a modern environment
822	at Silwood Lake, Silwood Park, Berkshire, England. Docs, U.S.G.P.O.f.s.b.t.S.o. Report.
823	Spicer, R.A., Wolfe, J.A., 1987. Plant taphonomy of late Holocene deposits in Trinity (Clair Engle) Lake,
824	northern California. Paleobiology 13, 227-245.
825	Spoth, M., 2020. Variations in the Southern Hemisphere westerlies over the last 23,000 years from lake
826	records in the Falkland Islands, Department of Earth Sciences. University of Maine.
827	Sprenger, M., Leistert, H., Gimbel, K., Weiler, M., 2016. Illuminating hydrological processes at the soil-
828	vegetation-atmosphere interface with water stable isotopes. Reviews of Geophysics 54, 674-704.

829	Thomas, E.K., Briner, J.P., Ryan-Henry, J.J., Huang, Y., 2016. A major increase in winter snowfall
830	during the middle Holocene on western Greenland caused by reduced sea ice in Baffin Bay and
831	the Labrador Sea. Geophysical Research Letters 43, 5302-5308.
832	Thomas, E.K., Hollister, K.V., Cluett, A.A., Corcoran, M.C., 2020. Reconstructing Arctic precipitation
833	seasonality using aquatic leaf wax $\delta^2 H$ in lakes with contrasting residence times.
834	Paleoceanography and Paleoclimatology 35, e2020PA003886.
835	Tipple, B.J., Berke, M.A., Doman, C.E., Khachaturyan, S., Ehleringer, J.R., 2013. Leaf-wax <i>n</i> -alkanes
836	record the plant-water environment at leaf flush. Proceedings of the National Academy of
837	Sciences 110, 2659-2664.
838	Tipple, B.J., Pagani, M., 2013. Environmental control on eastern broadleaf forest species' leaf wax
839	distributions and D/H ratios. Geochimica et Cosmochimica Acta 111, 64-77.
840	Toggweiler, J.R., Russell, J.L., Carson, S.R., 2006. Midlatitude westerlies, atmospheric CO ₂ , and climate
841	change during the ice ages. Paleoceanography 21.
842	West, A.G., Patrickson, S.J., Ehleringer, J.R., 2006. Water extraction times for plant and soil materials
843	used in stable isotope analysis. Rapid Communications in Mass Spectrometry 20, 1317-1321.
844	Wilkie, K.M.K., Chapligin, B., Meyer, H., Burns, S., Petsch, S., Brigham-Grette, J., 2013. Modern
845	isotope hydrology and controls on δD of plant leaf waxes at Lake El'gygytgyn, NE Russia. Clim.
846	Past 9, 335-352.
847	Williams, D.G., Ehleringer, J.R., 2000. Intra- and Interspecific Variation for Summer Precipitation Use in
848	Pinyon-Juniper Woodlands. Ecological monographs 70, 517-537.
849	Wyrwoll, KH., Dong, B., Valdes, P., 2000. On the position of southern hemisphere westerlies at the Las
850	Glacial Maximum: an outline of AGCM simulation results and evaluation of their implications.
851	Quaternary Science Reviews 19, 881-898.
852	
853	

Figure 1:

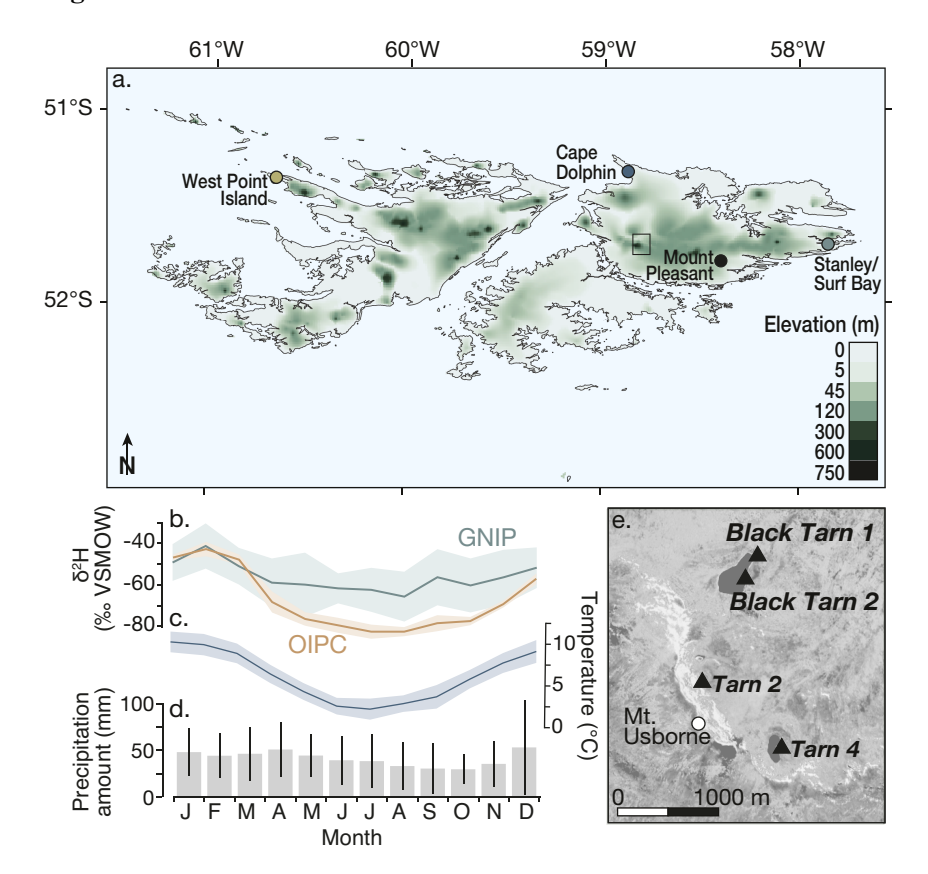


Figure 2:

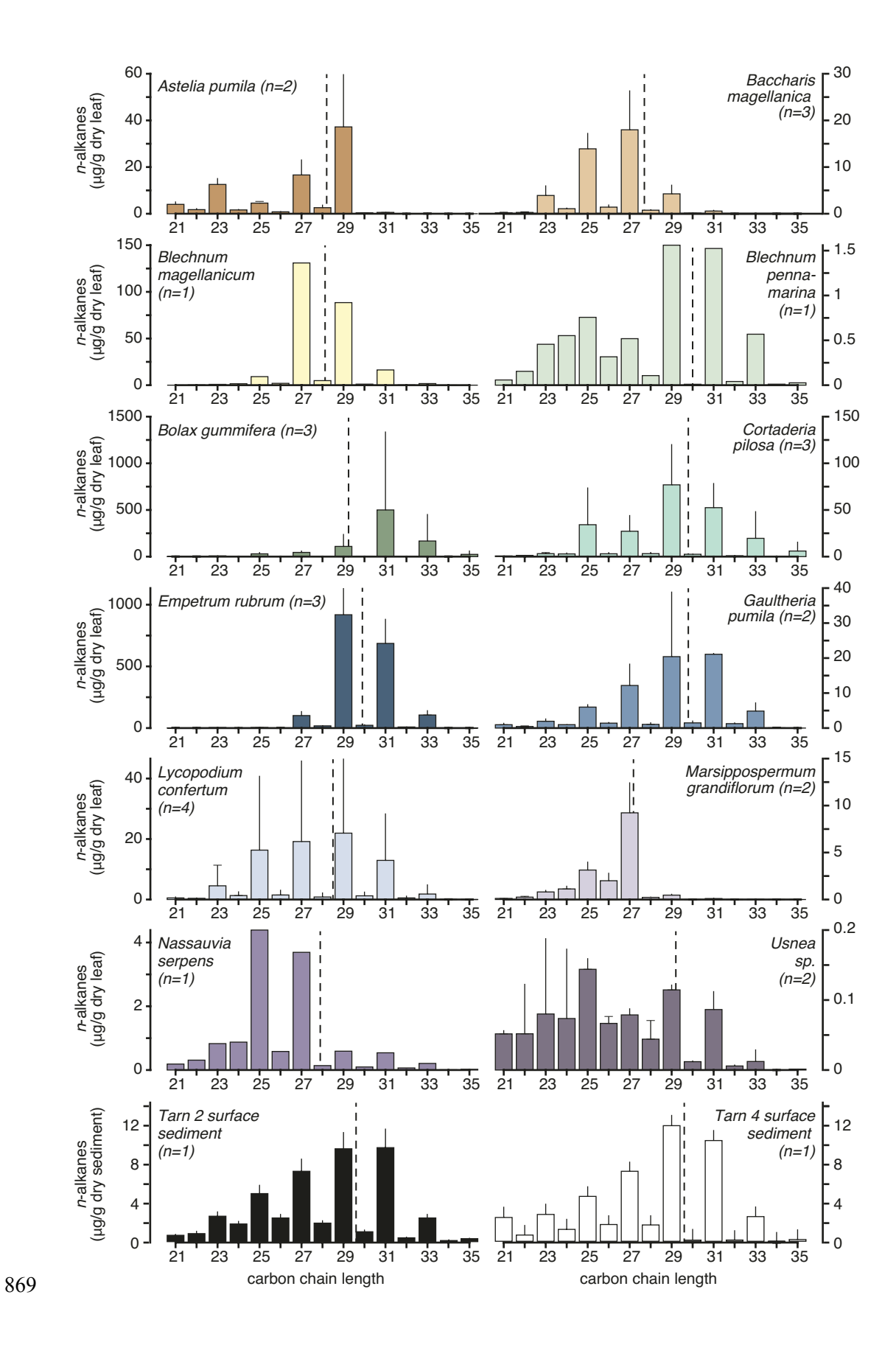


Figure 3:

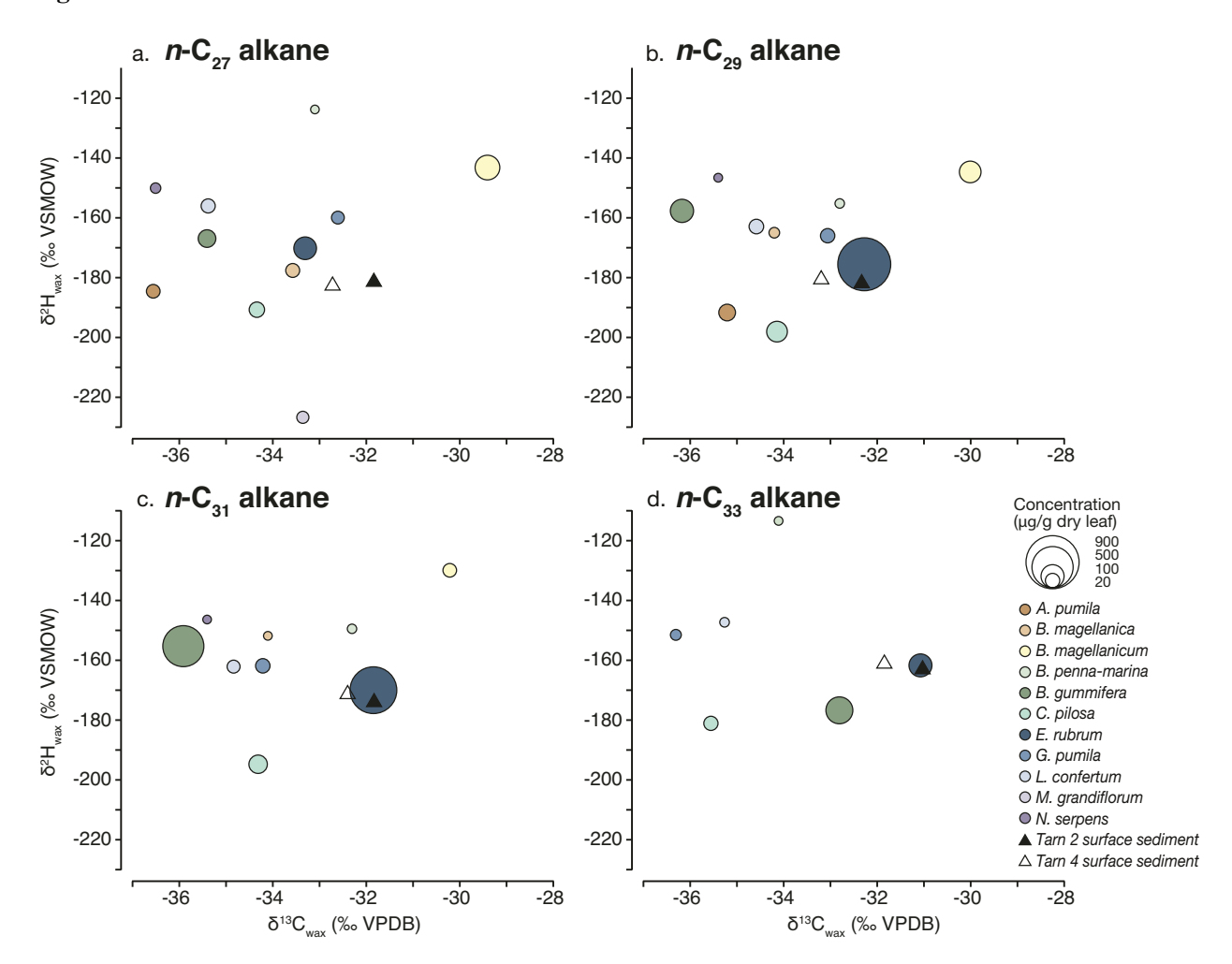


Figure 4:

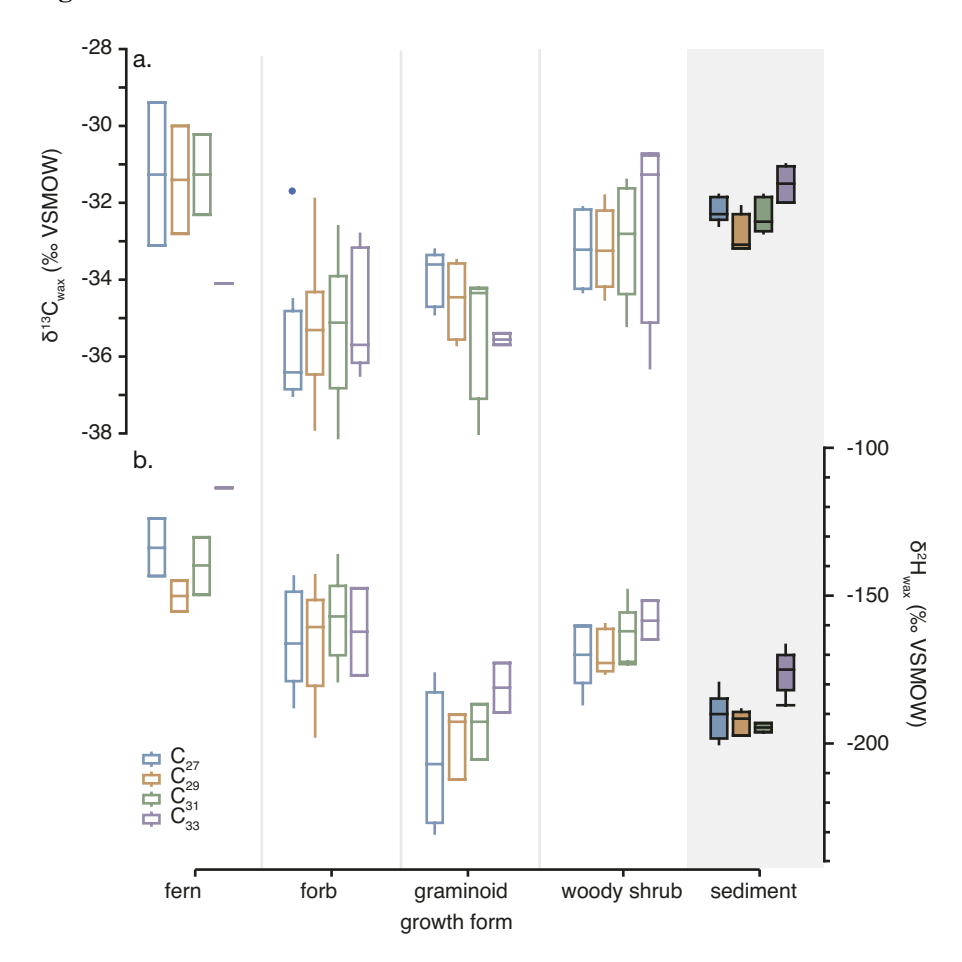


Figure 5:

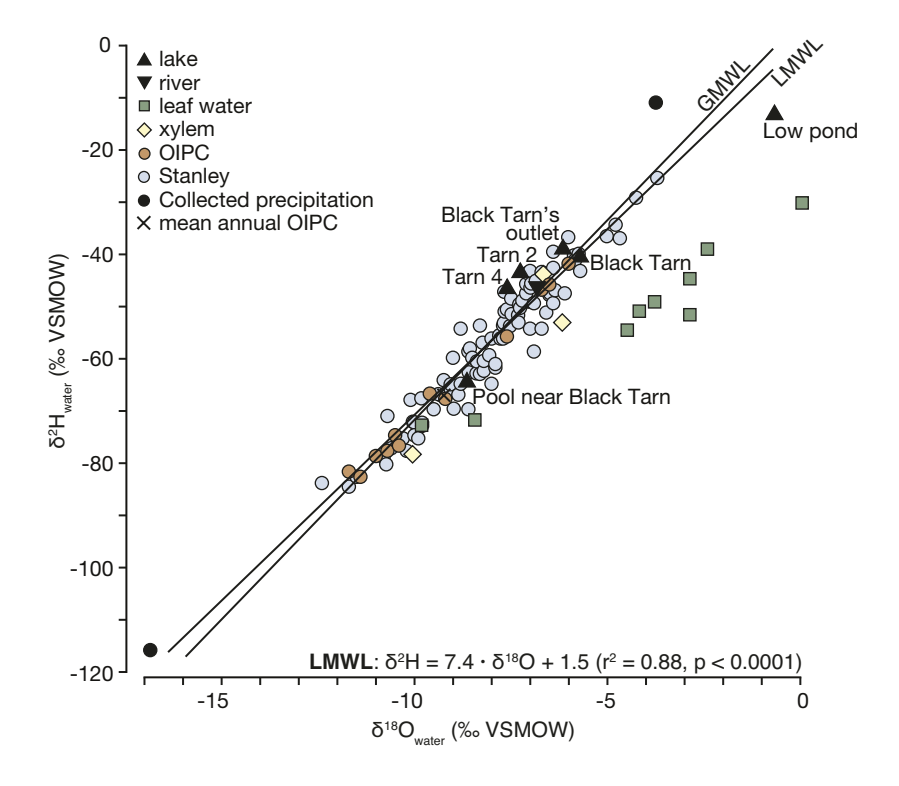


Figure 6:

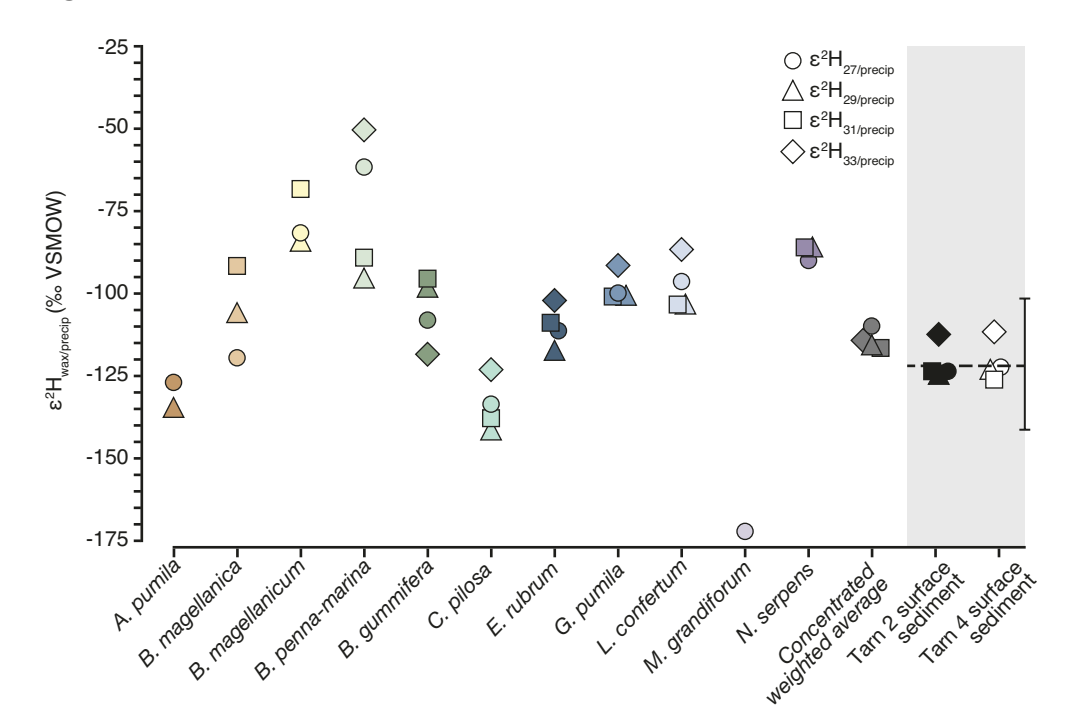


Figure Captions:

926

927

928

929

930

931

932

933

934

935

936

937

938

939

940

941

942

943

944

945

946

947

948

949

950

Figure 1: Map and modern climatology of the Falkland Islands. a) Elevation map of the Falkland Islands. Black dots indicate locations of precipitation isotope, temperature and precipitation amount data used in this study. Black box indicates map in panel e. b) Average monthly precipitation δ^2 H observed at Stanley (green) from 1961 to 1976 from the Global Network of Isotopes in Precipitation (GNIP), and monthly precipitation δ^2 H modelled at the sample collection sites (orange) from the OIPC (Bowen and Revenaugh, 2003; Groff et al., 2020; Bowen, 2021; IAEA/WMO, 2021). Modelled precipitation δ^2 H at each of the four collection sites is the same. Shaded region is the monthly standard deviation of precipitation $\delta^2 H$ determined at Stanley (green) and the 95% confidence interval for the modelled precipitation from the OIPC (orange). c) Average monthly temperature are from Mount Pleasant, FK for from 1985-2019 (NOAA, 2021). d) Average monthly precipitation amount from Mount Pleasant, FK from 1991 – 2019 (NOAA, 2021). e) Location of the four sampling locations and 3 neighboring lakes for this study. **Figure 2**: Abundances and chain length distributions for *n*-alkanes from 11 plants, 1 lichen species and 2 surface lake sediment from the Falkland Islands. Species examined for n-alkanes $C_{21} - C_{35}$ include A. pumila (n = 2), B. magellanica (n = 3), B. masellanicum (n = 1), B. penna-marina (n = 1), B. gummifera (n = 3), C. pilosa (n = 3), E. rubrum (n = 2), G. pumila (n = 2), L. conferta (n = 4), M. grandiflorum (n = 2)2), N. serperis (n = 1) and a lichen Usnea species (n = 2). Solid black lines are the standard deviation of all samples of that species. Vertical dashed lines indicate average chain length (ACL) for each species. Note each concentration axes are scaled individually to maximum chain length. Figure 3: Relationship between $\delta^2 H_{\text{wax}}$ and $\delta^{13} C_{\text{wax}}$ for each chain length for a-d) n- C_{27} , n- C_{29} , n- C_{31} , n-C₃₃ of the Falkland plant and surface lake sediment samples. Colors represent plant species and correspond to the colors in Fig. 2. Dot size indicates plant wax concentration. Surface lake sediment samples are shown as triangles. Analytical error on the concentration measurements is $\pm 2.0 \mu g/g$.

Figure 4: $\delta^{13}C_{\text{wax}}$ and $\delta^{2}H_{\text{wax}}$ for each of the plant growth forms studied, ferns (n = 2), forbs (n = 10), graminoids (n = 5), and woody shrubs (n = 8) and for sediment samples from Tarn 2 and Tarn 4 combined (n = 5) for n- C_{27} , n- C_{29} , n- C_{31} , n- C_{33} . a) $\delta^{13}C_{\text{wax}}$ b) $\delta^{2}H_{\text{wax}}$ Colors correspond to the carbon chain length. Boxes are quartiles about the median, whiskers are 5 and 95 percentiles and dots are outliers. Figure 5: Lake, river, leaf, xylem water and precipitation isotopes from the Falklands Islands. Symbols and colors correspond to different water types and locations. Lake water samples (black triangles) are labelled with which location the sample was collected from. Global meteoric water line (GMWL) and local meteoric water line (LMWL) are plotted. The LMWL was determined using the observed $\delta^2 H_{\text{precip}}$ and $\delta^{18}O_{\text{precip}}$ at Stanley (IAEA/WMO, 2020). **Figure 6**: Calculated fractionation, $\varepsilon^2 H_{27/precip}$, $\varepsilon^2 H_{29/precip}$, $\varepsilon^2 H_{31/precip}$ and $\varepsilon^2 H_{33/precip}$ of the Falkland plants and surface lake sediment. Colors represent plant species and correspond to the colors in Fig. 2. Symbols represent the chain length used to calculate $\varepsilon^2 H_{27\text{precip}}$ (circle), $\varepsilon^2 H_{29/\text{precip}}$ (triangle), $\varepsilon^2 H_{31/\text{precip}}$ (square) and $\varepsilon^2 H_{33/\text{precip}}$ (diamond). Weighted average of all plants for $\varepsilon^2 H_{27\text{precip}}$, $\varepsilon^2 H_{29/\text{precip}}$, $\varepsilon_{31/\text{precip}}$ and $\varepsilon^2 H_{33/\text{precip}}$ was calculated using chain length concentrations for each plant sample. Dashed line indicate global average $\varepsilon^2 H_{29/\text{precip}}$ (Sachse et al., 2012).

Site Name	Latitude (°S)	Longitude (°W)	Elevation (m)	δ ² H (‰ VSMOW)	δ ¹⁸ O (‰ VSMOW)
Black Tarn 1	51.6866	58.8202	385	-41	-5.7
Black Tarn 2	51.6850	58.8276	383	NA	NA
Tarn 2	51.6959	58.8276	600	-44	-7.3
Tarn 4	51.7022	58.8155	520	-47	-7.6
Pool near Black Tarn	51.6850	58.8194	383	-65	-8.6
Low Pond	51.6601	58.8327	63	-13	-0.7
River	51.6674	58.8172	73	-47	-6.8